12-2012

STUDY OF CELL VIABILITY DURING LASER DIRECT WRITING OF CELL-ALGINATE SUSPENSION

Hemanth Gudapati
Clemson University, hgudapati@hotmail.com

STUDY OF CELL VIABILITY DURING LASER-DIRECT WRITING OF CELL-ALGINATE SUSPENSION

A Thesis
Presented to
the Graduate School of
Clemson University

In Partial Fulfillment
of the Requirements for the Degree
Master of Science
Mechanical Engineering

---

by
Hemanth Gudapati
December 2012

Accepted by:
Dr. Yong Huang, Committee Chair
Dr. Jiro Nagatomi
Dr. Richard Figliola

ABSTRACT

Laser-assisted cell printing, developed based on Matrix-assisted pulsed-laser evaporation direct-write (MAPLE DW), a typical LIFT (laser-induced forward transfer) practice, has been emerging as one of the most promising biofabrication techniques. Alginate, particularly sodium alginate, is extensively used as the constituent of bioink in laser-assisted cell printing. However, thus far, studies investigating the effect of alginate gelation on cell viability in laser-assisted cell printing are lacking. The objective of this study is to investigate the effects of gelation, gelation time, sodium alginate concentration, and the effect of operating conditions such as the laser fluence on post-transfer cell viability during laser-assisted cell printing.

Two experimental setups have been designed in this study. Experimental setup A was characterized by laser fluences 800, 1200, and 1600 mJ/cm^2 and a constant alginate concentration of 1% w/v with 5 × 106 NIH3T3 cells/ml in bioink. Experimental setup B was characterized by alginate concentrations of 1, 2, and 3 % w/v with 5 × 10^6 NIH3T3 cells/ml in bioink and a constant laser fluence of 800 mJ/cm^2. Experimental setup A was designed to study the effects of gelation, gelation time, and laser fluence on post-transfer cell viability. Experimental setup B was designed to study effects of gelation and sodium alginate concentration on post-transfer cell viability. Furthermore, cell-laden alginate droplets were subjected to no gelation, two-minute gelation, or ten-minute gelation. Cell viability was evaluated immediately after printing and after 24 hours of incubation.

Process-induced cell injury during alginate gelation in laser-assisted cell printing is systematically elucidated through investigating the effects of operating conditions and

material properties on the post-transfer cell viability and cell injury reversibility. Two-minute gelation is observed to increase cell viability over 24 hours because of cushion effect. That is, forming gel membrane has minimized the impact of mechanical stresses generated during droplet landing. Despite ten minutes gelation having a cushion effect during droplet landing, it is observed to decrease cell viability over 24 hours because of the thick gel membrane which reduces nutrient diffusion from culture medium. Also, the longer exposure of encapsulated cells to calcium chloride has resulted in greater cell injury due to Ca^{2+} ions. Increase in laser fluence as well as alginate concentration is observed to decrease cell viability by introducing greater mechanical stresses during droplet formation. The process-induced cell death is modeled using power-law and Gompertz models. Gompertz model is observed to better predict cell viability than power-law model. However, the two models ignore molecular signaling pathways that govern the cell responses. Hence, future studies have to model process-induced cell death based on molecular signaling pathways.

DEDICATION

This thesis is dedicated to my family for their love and support.

ACKNOWLEDGMENTS

I wish to express my sincere thanks to my advisor, Professor Yong Huang, for providing this great opportunity and for his careful guidance. I would like to express my wholehearted gratitude to my other committee members, Professor Richard Figliola, Professor Jiro Nagatomi. I am very grateful to my fellow group member and dear friend Jingyuan Yan, and Wenxuan Chai for their help in this study. I would also like to thank Professor Nicole Coutris and my other group members Changxue Xu, and Leigh Herran.

TABLE OF CONTENTS

Page

Table of Contents (Continued)

Page

LIST OF TABLES

LIST OF FIGURES

List of Figures (Continued)

Figure Page

CHAPTER ONE

INTRODUCTION

1.1 Introduction

Organ transplantation is limited by hurdles such as pathogen transfer, immune rejection, and donor shortage. Tissue engineering aims to solve such limitations by applying the principles of biology and engineering to develop functional substitutes for damaged tissues and organs [Langer1993]. Tissue engineering consists of two types of manufacturing approaches, the traditional scaffold-based approach and the more recent scaffold-free approach. The scaffold-based tissue engineering approach is based on seeding of cells into biodegradable porous scaffolds. However, engineering of complex tissue constructs is still challenging in this approach. Cell adhesion, migration, and proliferation into scaffold are not effective and often difficult to control [Guillotin2011]. In addition, vascular networks required for blood circulation, nutrients supply, and waste removal are absent in scaffolds [Mironov2009, Guillotin2011].

The scaffold-free tissue engineering approach employs basic building blocks such as cell-laden microspheres to assemble larger functional three-dimensional (3D) tissue constructs through layer stacking, random packing, and 3D bioprinting [Mironov2009, Guillotin2011]. Because of its easy scale-up automation and precise simultaneous 3D positioning of different cell types, the scaffold-free approach addresses two main limitations of the scaffold-based approach, built in vascularization and controlled fabrication of complex tissue constructs [Mironov2009, Guillotin2011, Xu2012]. Among

various scaffold-free approaches, 3D bioprinting has emerged as one of the most promising tissue engineering approaches.

3D bioprinting is a layer-by-layer additive manufacturing technique. It takes advantage of rapid prototyping assisted by computer-aided design (CAD) and/or computer-aided manufacturing (CAM) procedures to build three-dimensional tissue constructs [Guillotin2011]. The 3D bioprinting strategies are primarily comprised of orifice-based and orifice-free techniques. Inkjet-based 3D cell printing is a major orifice-based technique. However, it suffers nozzle failure due to clogging, when printing highly viscous biomaterials. Laser-assisted 3D cell printing is a major orifice-free printing technique. Unlike ink jetting, laser-assisted cell printing is not restricted by viscosity constraints because of its orifice-free dispensing approach. Laser-assisted cell printing uses optical energy of laser beams for precise controlled deposition of materials. A typical laser-assisted printing setup in the biofabrication processes consists of a pulsed laser source, a bioink consisting of living cells to be transferred, a ribbon which is a laser transparent quartz disk coated with the bioink at one end, and a receiving substrate for the transferred cells.

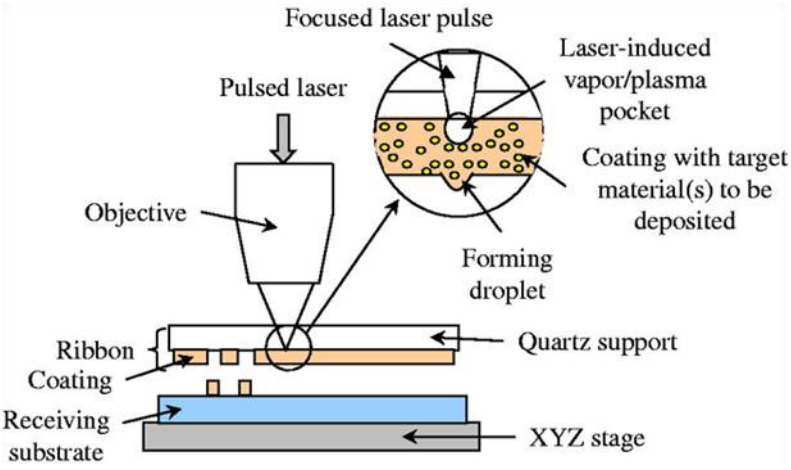

Figure 1.1: Laser-assisted printing setup [Lin2010]

When a laser beam is focused onto the backside of the ribbon, it generates a vapor bubble at the interface of the bioink coating and the quartz disk due to localized heating as shown in Figure 1.1. Subsequently, the vapor bubble expands rapidly and ejects a jet/droplet of the bioink into the receiving substrate. The receiving substrate is mounted on a moving stage controlled by a computer, to fabricate distinct 3D patterns of tissue constructs, out of the ejected droplets as shown in figure 1.1 [Lin2009a].

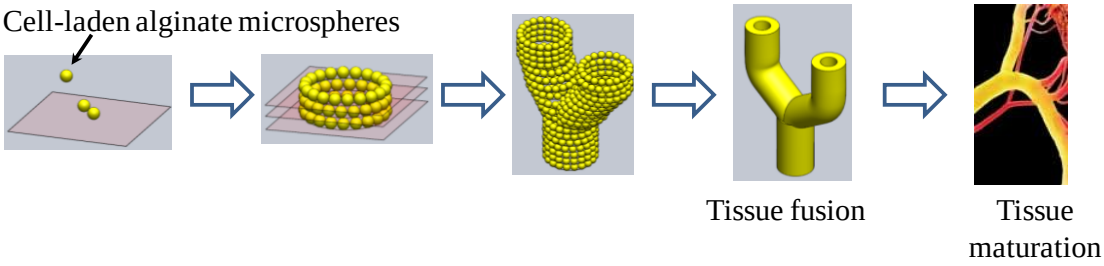

Figure 1.2: Fabrication of 3D vascular tree

1.2 Background

Alginate, particularly sodium alginate, is extensively used as the constituent of bioink 3D bioprinting printing processes to facilitate gelation [Khalil2006, Nishiyama2009, Xu2012]. Alginate upon gelation provides structural supports for tje 3D construct being fabricated as shown in Figure 1.2. In addition, gelled alginate acts as extra cellular matrix (ECM) for the encapsulated cells to attach, proliferate, and differentiate. Alginate primarily consists of a family of unbranched binary copolymers of 1,4 linked β-D-mannuronic acid (M blocks) and α-L-guluronic acid (G blocks) [Balandino1999, Rezende2007]. Alginate undergoes gelation when it interacts with divalent ions such as Ca^{2+}, Ba^{2+}, Fe^{2+}, and Sr^{2+} or trivalent ions such as Al^{3+}. The gelation occurs as the cations take part in the interchain ionic binding between G-blocks in the polymer chain giving rise to a more stable three dimensional network [Blandino1999, Mammarella2003, Rezende2007].

Incorporation of calcium chloride solution as a receiving substrate to induce alginate gelation in laser-assisted cell printing could be harmful to cells. Calcium ions are universal second messenger among cells and regulate vital cellular functions such as cell cycle regulation, proliferation, differentiation, gene expression, and cell death [Bernardi2007, Giorgi2008]. Alterations in intracellular as well as extracellular calcium ion concentrations have been reported to result in diverse cellular responses ranging from cell proliferation to cell death [Lee1992, Martino2011, McGinnis1999, McNeil1998]. Nature of response depends on cell type, concentration of calcium ions, and time duration of exposure of cells to calcium ions [Lee1992, McGinnis1999, McNeil1998].

In eukaryotic cells, intracellular (cytosolic) Ca^{2+} is maintained approximately at 100 nM while the extracellular Ca^{2+} is maintained nearly at 1 mM or more [Orrenius2003, Rizzuto2006]. Increase in extracellular Ca^{2+} has been reported to promote differentiation while inhibiting proliferation in mice epidermal cells (1.2 mM Ca^{2+}) and human breast epithelial cells (1.05 mM Ca^{2+}) [Hennings1980, Ochieng1991]. Meanwhile, Higher proliferation rates have been reported for rat fibroblast cells when extracellular Ca^{2+} is increased to 2 mM for 24hours [McNeil1998].

Contrastingly, an increase in extracellular Ca^{2+} to 5mM for 24 hours has been reported to cause death of SH-SY5Y human neuroblastoma cells [McGinnis1999]. Furthermore, hybridoma cell viability has been reported to decrease in mere few minutes (40 – 60 min) when extracellular Ca^{2+} was increased to 115-135 mM (1.3 – 1.5% w/v $CaCl_2$) [Lee1992]. Generally, a significantly large increase in extracellular Ca^{2+} concentration (1 – 2 % w/v $CaCl_2$) results in a lower cell proliferation rates [Xu2013] and even cell death [Lee1992].

1.3 Motivation and Objectives

Laser-assisted cell printing causes cell injury [Lin2009b, Lin2010a]. In addition, usage of calcium chloride solution as a receiving substrate could be injurious to cells [Lee1992, McGinnis1999, McNeil1998]. Challenges of laser-assisted cell printing include how to optimize operating conditions and which material properties to select for mitigating cell injury. Thus far, studies investigating cell injury during alginate gelation in laser-assisted cell printing are lacking. As a preliminary study towards the cell injury in laser-assisted 3D cell printing, this study serves to investigate the effects of alginate

gelation, gelation time, alginate concentration, and the effect of operating conditions such as the laser fluence on post-transfer cell viability during laser-assisted cell printing. In summary, this study tests the hypothesis that cell viability during alginate gelation in laser-assisted cell printing is affected by operating conditions and material properties especially gelation time, alginate concentration, and laser fluence.

This thesis is organized as follows. First, various studies on laser-assisted printing of different biomaterials are reviewed. Second, experimental setup and experimental design for cell viability test are given. Third, mechanisms of cell injury and modes of cell death in biofabrication processes including laser-assisted cell printing are outlined. Fourth, the process-induced cell injury is studied in two scenarios: immediately after printing and after 24 hours of incubation. Fifth, mathematical models for predicting post transfer cell viability in laser-assisted cell printing are derived using experimental results. Finally, the conclusions and future work are presented.

CHAPTER TWO

LASER-DIRECT WRITING OF VARIOUS BIOMATERIALS

2.1 Introduction

An overview of laser-assisted printing of various biomaterials by different research groups is outlined in this chapter. A vast majority of those studies are characterized by laser fluences lower than 800 mJ/cm^2 and reported minimal cell injury. However, fabrication of highly viscous cell-laden alginate microspheres requires laser fluences greater than 800 mJ/cm^2 [Lin2011]. In addition, laser fluences greater than 800 mJ/cm^2 cause cell injury [Lin2009b, 2010a]. Also, any observation made regarding cancerous cells by previous studies may not be applicable to healthy cells as cancerous cells are more resistant to cell death.

2.1.1 Proteins

Viability of laser-assisted printing for biofabrication processes was demonstrated by Ringeisen and colleagues in 2002 [Ringeisen2002]. A 193-nm laser pulse from an ArF excimer laser with a fluence of 50 mJ/cm^2 was used for dispensing proteins. Subsequent binding of proteins with their antigens demonstrated that laser printing did not damage the proteins. A typical cell not only consists of proteins but DNA, RNA, mitochondria, and other organelles which are essential for its functions. Furthermore, a very low laser fluence was used. Hence, any observation made regarding the laser-assisted printing of protein may not be applicable to other organelles as a whole.

2.1.2 Fungus

Hopp and colleagues undertook time-resolved photographic imaging of the laser-assisted cell printing process to evaluate ejected acceleration of trichoderma longibrachiatum conidia fungi [Hopp2005b]. The average acceleration of ejected conidia fungi was estimated to be $10^9 \times g$. A 248-nm laser pulse from a KrF excimer laser with fluence of 355 mJ/cm^2 and pulse duration of 30 ns was used for dispensing the fungi. The fungi were alive and were able to proliferate after printing.

Lin and colleagues investigated the effect of laser fluence on yeast cells viability [Lin2009b]. The yeast cell viability decreased from 80% to 50% when laser fluence was increased from 500 to 1500 mJ/cm^2. An important hypothesis was that printing process-induced cell injury was reversible and was a function of laser fluence. The cell population witnessed slight increase from immediately after printing to 24 hours after printing as the injured cells were repaired. This was based on the observation that control cell population did not witness any significant population increase.

An ArF excimer laser with wavelength of 193 nm, pulse duration of 12 ns, pulse repetition rate of 50 HZ, and laser spot size of 120×280 μm^2 was used. The laser fluence was varied between 85 – 1500 mJ/cm^2.The yeast cell concentration used was $4\text{-}5 \times 10^8$ cells/ml and the cell viability was assessed using methylene blue. Fungus unlike animal cells, possess cell walls. Hence, any observation made regarding the laser-assisted printing of fungi may not be applicable to animal cells.

2.1.3 Rat Cancer Cells

Functional viability of living cells after laser-assisted printing was demonstrated by Ringeisen and colleagues in 2004 with successful differentiation of P19 cells into the neural and muscle cell lineages [Ringeisen2004]. An excimer laser with wave length of 193 nm, fluence of 100 – 500 mJ/cm^2, pulse duration 30 ns, and spot size of 100 x 125 μm^2 was used for transferring P19 cells of concentration 1.5×10^7 cells/ml. Direct write height, the distance between the ribbon and the receiving substrate, was varied between 0.25 – 10 mm. The ribbon coating is composed of 100 μl of P19 cells deposited on Matrigel of thickness about 10-30 μm.

Cell viability was tested six hours post transfer using a live/dead viability/cytotoxicity (Molecular Probes L-3224) assay. In addition, alkaline and neutral comet assays were performed to detect single-strand breaks and double-strand breaks in DNA respectively for DNA damage analysis. Approximately 50% of the cells transferred onto a substrate with thinner hydrogel coating were alive whereas 95% of the cells transferred onto a substrate with thicker hydrogel coating were alive. Alkaline and neutral comet assay tests, which were performed on printed cells immediately and after 24 hours of incubation, showed negligible DNA damage.

Patz and colleagues fabricated three dimensional (3D) neural patterns by dispensing B35 neuronal cells to different depths within a partially polymerized Matrigel substrate by varying laser fluence [Patz2006]. Initially, a neuronal cell layer was deposited using a fluence of 80 mJ/cm^2. Subsequently, a second layer of cells was deposited on the first layer using a fluence of 50 mJ/cm^2. Finally, a third layer of cells

was deposited on the second layer using a fluence of 50 mJ/cm^2. TUNEL staining indicated that 97% of the cells were alive after 72 hours of printing and 3% of cells underwent apoptosis. An ArF pulsed excimer laser with wavelength of 193 nm was used. The direct write height was varied between 0.7 – 2 mm.

Doraiswamy and colleagues incorporated a triazene polymer absorbing layer as opposed to metallic sacrificial layer in their study [Doraiswamy2006]. Cell dispensing was achieved at much lower fluences which reduced the injury to the printed cells. The threshold fluence was observed to be 50 mJ/cm^2 for the cell transfer to occur and fluence of 70 mJ/cm^2 was used in the study as opposed to 150 mJ/cm^2 used in previous studies. An ArF pulsed excimer laser with wavelength of 193 nm, repetition rate of 10 Hz, duration of 30 ns, and spot diameter of 50 µm was used for dispensing rat B35 neuroblast clonal cells of concentration 1×10^7 cells/ml. The cell viability was investigated after 3, 6, 12, 24, and 48 hours post transfer.

2.1.4 Rat Normal Cells

Compatibility of laser-assisted printing for transfer of living cells was validated by Barron and colleagues in 2004 [Barron2004a]. Rat cells of concentrations 2-100 × 10^6 cells/ml were dispensed using laser-assisted printing to fabricate cellular stacks of 50-100 µm tall. An excimer laser with laser pulse of wavelength 193 nm and with fluence of 157 – 315 µJ/cm^2 was used for transferring the cells. The duration of the laser pulse used was 20 ns and the repetition rate was 100 Hz. The cells were tagged with a live/dead viability/cytotoxicity (Molecular Probes L-3224) assay and near 100% viability was observed up to four days.

Hopp and colleagues used time-resolved imaging to estimate the time duration for which the ejected droplets containing the cells accelerated [Hopp2005a]. The cells were observed to reach a constant velocity in 1μs and the acceleration of ejected droplets was $10^7 \times g$. A KrF excimer laser with wave length of 248 nm, fluence of 360 mJ/cm^2, and pulse duration of 30 ns was used for transferring the living cells. Rat Schwann, and rat astroglial cells of concentrations 2×10^6 cells/ml were used in the study. The cells were spread as a 140-160 μm thick layer on a quartz disk coated with a silver sacrificial layer of thickness 100 nm. The direct write height, the distance between the ribbon and the receiving substrate, used was 0.6 mm. Trypan blue which is a cell membrane impermeable assay was used for assessing the cell viability. Approximately 98-99% of cells were alive before printing and 80-85% of cells were alive after printing.

2.1.5 Mouse Embryonic Stem Cells

Kattamis and colleagues employed a thick polymer absorbing sacrificial layer for printing mouse embryonic stem cells [Kattamis2007]. The thickness of polymer absorbing layer was greater than laser absorption depth and the polymer layer insulated the cells from thermal and mechanical shocks. Nearly all printed cells when observed with an optical microscope were found to be viable.

2.1.6 Sheep Normal Cells

Ovsianikov and colleagues employed laser-assisted printing for seeding two-photon polymerization (2PP)-fabricated scaffold with sheep endothelial cells (ECs) and vascular smooth muscle-like cells (vSMCs) [Ovsianikov2010]. In this approach

propulsive force generating from the laser-induced shockwave was used to propel individual cells or group of cells into the scaffolds. The cell concentrations used were 3.4 × 10^6 cells/ml for endothelial cells and 1.8 × 10^6 cells/ml for and vascular smooth muscle-like cells. Before printing, the cells were centrifuged and suspended in the alginate-blood plasma hydrogel and subsequently seeded on to the scaffolds.

No damage with regard to genotype and phenotype was observed in the seeded cells. A solid-state Nd:YAG-laser with wavelength of 1064 nm, pulse duration of 8-9 ns, and repetition rate of 20 Hz was used for printing. Gold layer with thickness of 55-60 nm was used as a sacrificial layer. The cells were applied onto the gold layer to form a layer of thickness 50 µm.

2.1.7 Pig Normal Cells

Hopp and colleagues used pig lens epithelial in addition to rat Schwann, and rat astroglial cells to estimate acceleration time of the ejected droplets containing the cells [Hopp2005a]. Pig lens epithelial cells of concentrations 2 × 10^6 cells/ml were used in the study. The cells were spread in a 140-160 µm thick layer on a quartz disk coated with silver layer of thickness 100 nm. The direct write height used was 0.6 mm. Approximately 98-99% of cells were alive before printing and 80-85% of cells were alive after printing.

2.1.8 Human Cancer Cells

Barron and colleagues used human osteosarcoma, in addition to rat cells, to fabricate cellular stacks of 50-100 µm tall [Barron2004a]. An excimer laser with laser

pulse of wavelength 193 nm and with fluence of 157 – 315 μJ/cm^2 was used for transferring the cells. The duration of the laser pulse used was 20 ns and the repetition rate was 100 Hz. The cells were tagged with a live/dead viability/cytotoxicity (Molecular Probes L-3224) assay and near 100% viability was observed up to four days.

Improved cell viability was achieved by Barron and colleagues in 2004 by using a laser absorbing interlayer or sacrificial layer between the quartz disk and the living cells [Barron2004b]. The printing process was called as biological laser printing (BioLP). Gold of thickness 35 nm, titanium of thickness 75 nm, and titanium dioxide of thickness 85 nm were used as absorbing layers. A 193-nm laser pulse with duration of 20 ns from an ArF excimer laser with fluence of 160 mJ/cm^2 was used for dispensing the living cells. The cells used were human osteosarcoma cells of concentration 1.5×10^8 cells/ml and mouse endothelial cells of concentration 4×10^7 cells/ml. The receiving substrate was coated with 50 – 200 μm of Matrigel. The cells were tagged with a live/dead viability/cytotoxicity (Molecular Probes L-3224) assay and near 100% viability was observed for 6-20 hours post transfer.

Barron and colleagues in a similar study estimated droplet deceleration to be 2×10^6 m/s^2 when it impacted the receiving substrate based on an initial velocity of 10 m/s and deceleration time of 4 μs [Barron2004c]. However, in spite of large deceleration forces, nearly 95% of cells were found to be viable 24 hours after printing. A Nd : YAG laser with wave length of 266 nm, fluence of 191 – 382 mJ/cm^2, and pulse repetition rate of 1-15 Hz was used for transferring human osteosarcoma cells of concentration 1×10^8 cells/ml.

In another similar study, minimal expression of heat shock proteins by printed cells was demonstrated suggesting that the minimal protein damage due to laser-assisted cell printing [Barron2005]. A 248 nm laser pulse with duration of 2.5 ns and repetition rates of up to 100 HZ from a PSX-100 excimer laser with fluence of 25-90 mJ/cm^2 was used for dispensing the living cells. The cells used were human osteosarcoma cells of concentration 1×10^7 cells/ml which were printed onto a microscope slide coated with a 50-μm thick layer of hydrogel.

Co-deposition of living cells, extracellular matrix (ECM), and bioceramic scaffold materials was investigated by Doraiswamy and colleagues [Doraiswamy2007]. In general, ECM contains growth factors and provides structural support for cells to attach, proliferate, and differentiate. Human osteosarcoma cells of concentration 1×10^7 cells/ml were used in the study. Nearly 100% of the printed cells were viable and were able to differentiate. An ArF excimer laser with wave length of 193 nm, fluence above 150 mJ/cm^2, and pulse repetition rate of 10 Hz was used for transferring the living cells.

In another study, Lin and colleagues investigated effect of laser fluence on human colon cancer cells viability [Lin2010]. The colon cancer cell viability decreased from 90% to 75% when laser fluence increased from 250 to 1500 mJ/cm^2. The colon cancer cell concentration used for printing was 1×10^7 cells/ml and 20 μl of cell suspension of the cells was applied on the quartz disc resulting in 80-100 μm thick layer. Trypan blue assay was used for assessing the cell viability immediately after printing. An ArF excimer laser with wavelength of 193 nm, pulse duration of 12 ns, pulse repetition rate of 50 Hz, and laser spot size of 120×280 μm^2 was used.

2.1.9 Human Normal Cells

Effect of laser energy, bioink viscosity (sodium alginate concentration), and substrate film thickness on viability of human endothelial cells in laser-assisted printing was evaluated by Catros and colleagues [Catros2011]. Cell viability decreased as laser energy increased from 8 µJ to 24 µJ. More cells were dead when the cells were printed using 8 µJ laser energy on to a substrate coated with 20 µm thick Matrigel coating than onto a substrate with 40 – 100 µm thick Matrigel coating.

Effect of bioink viscosity was evaluated by using 0.5% and 1% (w/v) sodium alginate. Subsequently, cells were printed using different laser energies of 12µJ, 18 µJ, and 24 uJ on to a substrate with 40 µm thick Matrigel coating. Cell viability was observed to improve with increase of sodium alginate concentration or bioink viscosity and was independent of variations in laser energy.

A Nd:YAG laser with 1064 nm wavelength, 30 ns pulse duration, and 5000 Hz repetition rate was used for printing. A Gold layer of thickness 50 nm was used as the absorbing sacrificial layer and the direct write height was set at 500 µm. Cells of concentration 1×10^7 cells/ml were suspended with either 0.5% or 1% (w/v) sodium alginate and were used as the bioink.

2.1.10 Human Stem Cells

Koch and colleagues evaluated impact of laser-assisted printing on cell survival, proliferation, apoptosis, DNA damage, and phenotype changes [koch2009]. Fibroblasts (NIH3T3), keratinocytes (HaCaT), and human mesenchymal stem cells (hMSC) were used for fabricating different 2D patterns consisting of one or more cell types. Nearly

98% of skin cells and 90% of stem cells survived the transfer immediately after printing. Caspase 3/7 activity was evaluated at 12 h, 24h, and 48 h post printing for apoptosis evaluation. All cell types showed negligible elevated caspase 3 activity at each of the time intervals when compared to control cells. DNA damage was assessed by using comet assay method and there was no significant increase in the DNA damage in comparison with the control cells.

A Nd:YAG laser with 1064 nm wavelength, 8–9 ns pulse duration, and 20 Hz repetition rate was used for printing. The laser fluence was varied between 3000 – 6000 mJ/cm^2. All cell lines were suspended in blood plasma and alginate hydrogel which resulted in a bioink of 1-2 × 10^6 cells/ml in 30 µL. Gold was used as the absorbing layer and the direct write height is set between 350-500 µm. The coating thickness was 50 µm.

In one study Gruene and colleagues fabricated 3D-grid shaped grafts with human adipose-derived stem cells and alginate-blood plasma hydrogel as matrix material [Gruene2011c]. The graft height was about 240 µm and the height of each printed layer of the cells was about 40 µm. Generation of 3D grafts was achieved in three steps. Initially, alginate was blade coated on top of the collector slide and subsequently subjected to gelation through calcium chloride cross-linking.

Later, three layers of cell containing hydrogel were dispensed onto the collector slide. Finally calcium chloride was spray coated over the printed cell layers and the construct was placed in an incubator for several minutes for gelation. Human adipose-derived stem cells at passages 5–6 were used for this study and the printed cells were

subjected to adipogenic differentiation post transfer over a period of 21 days. The proliferation of printed cells and non-printed control cells was identical.

2.2 Summary

Laser-assisted printing technique has been investigated because of its advantage in printing viscous materials. The effects of process parameters on cell injury and cell viability during the printing process have also been widely studied. Process parameters in laser-assisted cell printing include operating conditions, such as laser fluence, direct writing height and receiving substrate thickness, and incubation time. Lin and colleagues [Lin2009b] [Lin2010a] studied the effect of laser fluence on yeast cell and human colon cancer cell viabilities, and found that the cell viabilities decrease with laser fluence for both cells. The effect of direct writing height in laser-assisted printing has also been evaluated [Lin2010b], and there was no noticeable viability difference under low laser fluences, but obvious viability improvement with direct writing height under large laser fluences. Effect of matrigel coating thickness of the receiving substrate on the post-transfer mammalian cell viability has been studies by Ringeisen and colleagues [Ringeisen2004], and cell viability increases with substrate film thickness. The effect of incubation time on cell viability has also been investigated. Barron and colleagues [Barron2005] studied the cell proliferation during 6 days of incubation for single cell printing. Lin and colleagues [Lin2010] investigated the post-transfer cell proliferation after 24, 48 and 72 hours of incubation. Other factors that may affect the cell injury and cell viability are thermal injury and UV radiation injury, etc., which are not considered as important during laser-assisted printing [Lin2009b].

Furthermore, sodium alginate was also incorporated as the matrix material for cells in further studies of laser-assisting printing. Though alginate is not an ideal material for living tissue reconstruction because of its low cell adhesiveness and poor support of cell proliferation [Yao2012], it is a good material for proof-concept-studies [Xu2012]. Among the studies on laser-assisted cell printing that incorporate as bioink, Guillemot and colleagues [Guillemot2010] demonstrated the potential of using high-throughput biological laser printing technique to create well-defined nano-sized cell patterns. Catros and colleagues [Catros2011] studied the effect of laser fluence on endothelial cell viability, and it is also found that the cell viability decrease with laser fluence. It is also found that the cell viability increase with receiving substrate thickness as well as bioink viscosity.

Unfortunately, though bioink that incorporates sodium alginate has been applied, studies investigating the effect of alginate gelation on cell viability in laser-assisted cell printing are lacking. This study aims to understand the influence of alginate gelation on cell viability in laser-assisted cell printing. Cells together with different concentrations of sodium alginate solutions are printed. Calcium chloride is used as substrate solution for printed cells, and the post-transfer cell viability with different gelation times under various laser fluences are evaluated. In this study, post-transfer cell viability after 24 hours of incubation is tested and is of particular interest more than that of post-transfer cells after 0 hour, since the reversibility of process-induced cell injury can mostly be completed within the first day of incubation, and it is of more significance in cell printing researches.

CHAPTER THREE

EXPERIMENTAL DESIGN

3.1 Introduction

Two experimental setups have been designed in this study to investigate the effects of gelation, gelation time, sodium alginate concentration, and the effects of operating conditions such as the laser fluence on post-transfer cell viability during laser-assisted cell printing. Experimental setup A was characterized by laser fluences 800, 1200, and 1600 mJ/cm^2 and a constant alginate concentration of 1% w/v with 5×10^6 NIH3T3 cells/ml in bioink. Experimental setup B was characterized by alginate concentrations of 1, 2, and 3 % w/v with 5×10^6 NIH3T3 cells/ml in bioink and a constant laser fluence of 800 mJ/cm^2. Experimental setup A was designed to study the effects of gelation, gelation time, and laser fluence on post-transfer cell viability. Experimental setup B was designed to study the effects of gelation and sodium alginate concentration on post-transfer cell viability. The experimental design process is described in this chapter.

3.2 Experimental Setup

Matrix-assisted pulsed-laser evaporation direct-write (MAPLE DW), a typical LIFT (laser-induced forward transfer) practice [Lin2009a] [Yan2012], has been of particular interest in this study for cell printing. As shown in Figure 3.1, the experimental setup consisted of an ArF excimer laser (Coherent ExciStar, Santa Clara, CA) with wavelength of 193 nm and 12 ns (full-width half-maximum). The laser fluence was

measured using a Coherent FieldMax power/energy meter (Coherent, Portland, OR). The laser spot size diameter was maintained at150 μm whereas the laser repetition rate was maintained at 30 Hz. The bioink was comprised of sodium alginate solution and NIH3T3 cells to be transferred. Quartz disk (Edmund optics, Barrington, NJ) with 85% transmittance for 193 nm wavelength laser beams was used to make the ribbon, which had the bottom side coated with the bioink. A teflon tape (3M, St. Paul, MN) was applied on the bottom side of the quartz disk to make a 1.5 × 1.5 cm square well. Each time, 20 μL of the bioink was pipetted onto the quartz disk well and was spread evenly to produce an 80-100 μm thick layer. The receiving substrate for the transferred cells, which consisted of a substrate container and a substrate liquid, was made of a 24-well plate with one well containing either 1 ml of Dulbecco's Modified Eagles Medium (DMEM) or 1 ml of calcium chloride.

The laser beam, when focused onto the backside of the ribbon, immediately generated a vapor bubble at the interface of the bioink coating and the quartz disk due to localized heating. Subsequently, the vapor bubble expanded rapidly and ejected a jet/droplet of the bioink into the receiving substrate. Ejected sodium alginate jets/droplets containing the cells were subjected to gelation when printed into the substrate container containing the calcium chloride. Whereas, the droplets were not subjected to gelation when printed into the substrate container containing the DMEM culture medium. The direct writing height, which is the distance between the ribbon and the liquid level in substrate container, was 1 mm. The receiving substrate was mounted onto XY translational stages (Aerotech, Pittsburgh, PA). The ribbon and the receiving substrate

were relative immobile, and the relative motion between the laser beam and the receiving substrate was set at 300 mm/min and was controlled using a computer.

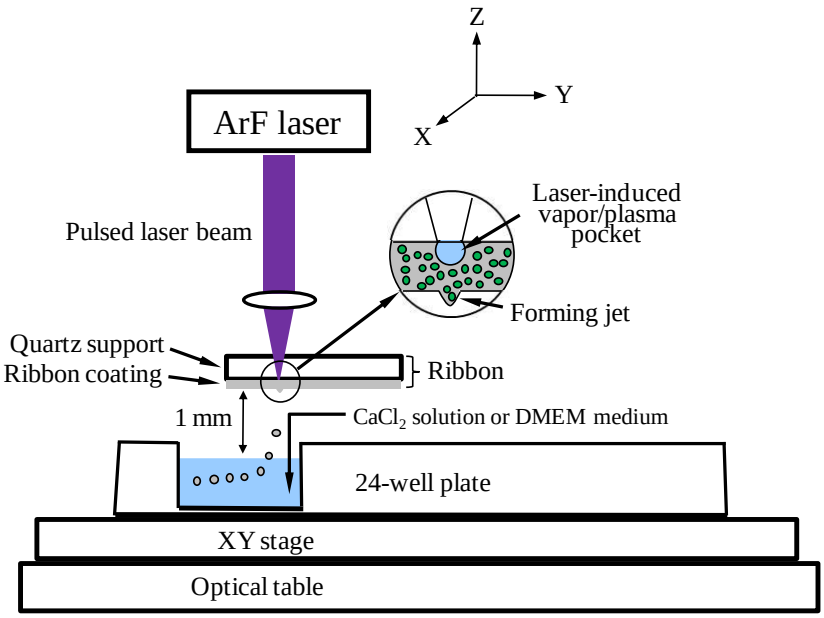

Figure 3.1: Schematic of laser-assisted cell printing experimental setup

3.3 Materials and Methods

3.3.1 Bioink Preparation

The bioink is primarily comprised of sodium alginate solution and NIH3T3 mouse fibroblast cells. The cells were cultured in DMEM (Sigma Aldrich, St. Louis, MO) supplemented with 10% Fetal Bovine Serum (FBS) (HyClone, Logan, UT) in a humidified 5% CO_2 incubator (VWR, Radnor, PA) at 37°C, and the culture medium was replaced every three days as required. Freshly confluent flasks of 3T3 fibroblasts were washed twice with Dulbecco's phosphate-buffered saline (PBS) (Cellgro, Manassas, VA), and incubated with 0.25% Trypsin/EDTA (Sigma Aldrich, St. Louis, MO) for 5 min at 37°C to detach the cells from the culture flasks. Then the cell suspension was

centrifuged at 1000 rpm for 5 minutes at room temperature, and the resulting pellet was resuspended in DMEM complete cell culture medium. The resuspended cells were adjusted to the cell concentration of 1×10^7 cells/ml.

Three different concentrations of sodium alginate solution were used in the study. Sodium alginate powder (Sigma-Aldrich, St. Louis, MO) was mixed with DMEM culture medium to obtain 2%, 4%, and 6% (w/v) of sodium alginate solution respectively. Each concentration of sodium alginate solution was mixed with NIH3T3 cells at a 50-50 percent volume ratio to obtain 1%, 2%, and 3% (w/v) of bioink with 5×10^6 cells/ml.

3.3.2 Ribbon preparation

Quartz disks with 85% transmittance for 193 nm wavelength laser beams were used as part of the ribbons. Initially, the quartz disks were cleaned with an ultrasonic cleaner (Branson, Danbury, CT) and de-ionized water for five minutes. The quartz disks were then rinsed with 70% ethanol. Later, the quartz disks were washed with water and were air dried. Then the quartz disks were sterilized using an ultraviolet lamp for 15 minutes on the side that was coated with bioink. Thereafter, a 3M Teflon tape was used to make a 1.5 × 1.5 cm square well with approximately 100 µm depth. Finally, 20 µL of the bioink was pipetted into the quartz disk well and was spread evenly to produce an 80-100 µm thick layer.

3.3.3 Receiving substrate preparation

A 24-well plate containing either DMEM culture medium or calcium chloride solution was used as the receiving substrate. The well plate was cleaned with a process

similar to that used for cleaning quartz disks. Briefly, the cleaning process involved ultrasonic cleaner, distilled water, 70% ethanol, and air drying. Calcium chloride dihydrate (Sigma-Aldrich, St. Louis, MO) was used for making 2% (w/v) calcium chloride solution. A single well of the well plate was filled with either 1 ml of calcium chloride or 1 ml of DMEM culture medium and was used as the receiving substrate for the printed bioink jets/droplets. During the printing process, alginate jets/droplets undergo gelation during the impact with calcium chloride solution. The gelation occurs because of the osmosis of calcium ions into the alginate microspheres [Cao2012].

3.3.4 Evaluation of cell viability

The testing solution used for evaluating the cell viability was 0.4% trypan blue stain (Biowhittaker, Walkersville, MD). Under in vitro culture conditions, apoptotic cells and their apoptotic bodies lyse in a process similar to necrosis as phagocytic cells are normally absent. This is known as secondary necrosis or post-apoptotic necrosis [Zhivotovsky11]. As a result, trypan blue which is a plasma membrane impermeable dye was sufficient to detect apoptotic as well as necrotic cells. Post-transfer cell suspension and trypan blue dye were mixed at a 50-50 percent volume ratio to make a testing sample. The sample was pipetted onto a hemocytometer (Hausser Scientific, Horsham, PA) and then was viewed using an optical microscope. Figure 3.2 shows a sample of live and dead cells under microscopic view. For the cells with intact cell membrane, the blue indicator turned bright and colorless in the presence of active enzymes, thus indicating live cells. For the cells with permeable cell membrane, the blue stain remained inside the

cells, indicating dead cells. Thereafter, the live and the dead cells were counted under the microscope.

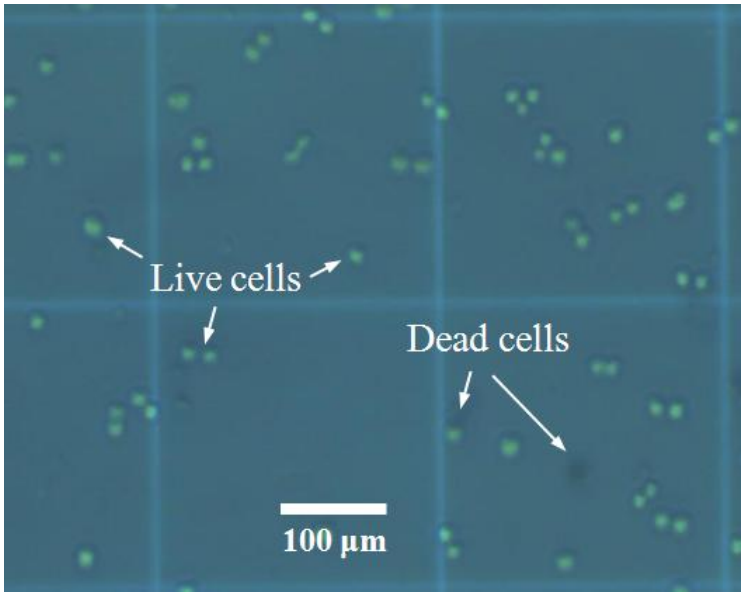

Figure 3.2: Post-transfer NIH3T3 cells stained with trypan blue

Specifically, the following samples have been tested: bioink printed into DMEM medium as well as bioink printed into calcium chloride solution at two minutes gelation and ten minutes gelation, immediately after printing and after 24 hours of incubation. The NIH3T3 cells from the alginate bioink which were not applied onto the ribbon were subjected to no incubation and 24 hours of incubation, and were used as the control cells for non-incubated samples and incubated samples respectively.

The testing sample is made of cell sample/suspension and trypan blue dye mixed at 1:1 volume ratio. The cell sample/suspension preparation differs as some cells were subjected to gelation while others were not subjected to gelation. For cells subject to no gelation, the cell sample/suspension preparation protocol is as follows: the DMEM medium with printed bioink droplets in substrate container was pipetted into a centrifuge

tube, and then centrifuged for two minutes at 1100 rpm. Then, the supernatant solution was carefully pipetted out, leaving cells with small amount of liquid at the bottom of the centrifuge tube to make the cell sample/suspension. If incubation is needed, the solution in substrate container was pipetted into a Petri dish containing 0.5 ml DMEM medium instead of pipetting into a centrifuge tube. Then the Petri dish was incubated for 24 hours in an incubator containing 5% CO_2 at 37 °C. After 24 hours of incubation, the cells were detached by trypsinization, prior to evaluation of the viability. The trypsinization process can be briefly described as, first, DMEM medium was pipetted out into a centrifuge tube from the Petri dish. Second, cells in the Petri dish were washed with the DPBS solution and third, 0.5 ml of 0.25% Trypsin-EDTA solution was added to the culture dish. Fourth, the cells in the Petri dish together with the Trypsin-EDTA solution were incubated for 3-5 minutes. Fifth, the cells and the Trypsin-EDTA solution were pipetted into the same centrifuge tube which contained the earlier pipetted out DMEM medium. After completing the trypsinization process, the centrifuge tube was centrifuged and cell viability was evaluated.

For cells subjected to gelation, the cell sample/suspension preparation protocol is as follows: the calcium chloride with gelled bioink microsperes in substrate container was pipetted into a centrifuge tube, and then centrifuged for two minutes at 1100 rpm. Thereafter, supernatant calcium chloride solution was pipetted out of the centrifuge tube, leaving concentrated gel at the bottom of the centrifuge tube. Gelled alginate hydrogel microspheres containing NIH3T3 cells were liquefied post-transfer to assess the cell viability. To liquefy the concentrated gel, 0.5 ml of 0.055 M sodium citrate solution was

added to the centrifuge tube. The gel was allowed to interact with sodium citrate for one minute to complete liquification. The resulting solution inside the centrifuge tube was then centrifuged for two minutes at 1100 rpm. Then, the supernatant sodium citrate solution was pipetted out, leaving cells with small amount of liquid at the bottom of the centrifuge tube. If incubation is needed, the concentrated gel was transferred out of the centrifuge tube into a Petri dish containing 1.5 ml of DMEM medium. Then the gel was incubated for 24 hours in an incubator containing 5% CO_2 at 37 ℃. After 24 hours of incubation, the gelled droplets were liquefied and cell viability was evaluated.

3.3.5 Design of experiments

Effect of alginate gelation on cell viability was investigated immediately after printing and after 24 hours of incubation in this study. The effect of gelation was studied by comparing the viabilities of the cells in the bioink that was printed into calcium chloride solution with the viabilities of cells in the bioink that was printed into DMEM medium. The experiments were characterized by four important parameters: gelation time, laser fluence, sodium alginate concentration, and incubation time. The gelation times studied in the experiment were two minutes and ten minutes. Three different laser fluences (800, 1200 and 1600 mJ/cm^2) were used in the experiments. The concentrations of the sodium alginate solution comprising NIH3T3 cells were 1%, 2%, and 3% (w/v) respectively.

During the gelation, printed alginate droplets were allowed to interact with calcium chloride solution for two minutes or ten minutes after printing. Two minutes gelation time was chosen as it was the least possible time that could be used in this study.

Whereas, ten-minute gelation condition was chosen as the gel membrane thickness of the microspheres reaches nearly 100% of its maximum value within the first ten minutes of gelation [Blandino1999]. Since cells were mostly repaired than proliferated within the first 24 hours of incubation, and incubated cells are of more importance in cell printing researches, post-transfer cell viability after 24 hours of incubation are of interest in this study than cell viability immediately after printing.

Table 3.1: Experimental design

Setup	A	B
NaAlg concentration (w/v)	1%	1%, 2%, 3%
Laser fluence (mJ/cm^2)	800, 1200, 1600	800
Gelation time (min)	2, 10	2
Cell concentration (cells/ml)	5×10^6	
Receiving substrate	2% (w/v) $CaCl_2$, DMEM Medium	
Incubation time (h)	0, 24	
Control	Cells from unprinted bioink	

Two experimental setups were used as shown in Table 3.1 for assessing the effects of various parameters in laser-assisted printing process on cell viability. Experimental setup A was used for investigating the effects of gelation, gelation time as well as laser fluence on post-transfer cell viability. Experimental setup B was used for

examining the effects of gelation and sodium alginate concentration on post-transfer cell viability.

In Experimental setup A, a single concentration of sodium alginate in bioink which is 1% (w/v) with 5×10^6 cells/ml was used. The laser fluences used were 800, 1200, and 1600 mJ/cm^2. Two receiving substrate solutions, which were 2% (w/v) calcium chloride solution and DMEM culture medium, were used for each of the three laser fluences. Alginate droplets printed into the calcium chloride solution underwent gelation whereas alginate droplets printed into DMEM media did not undergo gelation. The incubation periods used were 0 hour and 24 hours after printing.

In Experimental setup B, two different sodium alginate concentrations in bioink were used which were 2% and 3% (w/v) with 5×10^6 cells/ml respectively. A laser fluence of 800 mJ/cm^2 was used for printing the bioink. Either 2% (w/v) calcium chloride solution or DMEM medium were used as the receiving substrate same as in Experimental setup A. The incubation periods used were 0 hour and 24 hours after printing.

3.4 Summary

Two experimental setups have been designed in this study to investigate the effects of gelation, gelation time, sodium alginate concentration, and the effects of operating conditions such as the laser fluence on post-transfer cell viability during laser-assisted cell printing. In the two experimental setups, cell viability was assessed immediately after printing as well as after 24 hours of incubation. Furthermore, cell-laden alginate droplets were subjected to no gelation, two-minute gelation, or ten-minute gelation. No gelation condition was one in which alginate droplets were printed into

DMEM culture medium. Two minutes gelation condition was in one which alginate droplets were allowed to interact with calcium chloride solution, the receiving substrate, for two minutes. Similarly ten-minute gelation condition was in one which alginate droplets were allowed to interact with calcium chloride solution for ten minutes. Two minutes gelation time was chosen as it was the least possible time that could be used in this study. Whereas, ten-minute gelation condition was chosen as complete gelation of droplets occurs within 3-4 minutes.

CHAPTER FOUR

MECHANISMS OF PROCESS-INDUCED CELL INJURY

4.1 Introduction

An injury to a cell, resulting because of biofabrication processes including laser-assisted cell printing, is often referred to as process-induced cell injury. Process-induced cell injury in laser-assisted cell printing is of three types, mechanical cell injury, thermal cell injury, and chemical cell injury. Mechanical cell injury is caused by mechanical stresses generated during the droplet formation and during the droplet landing processes. Similarly, thermal cell injury is caused because of optical heating by laser pulses. However, it has been reported that laser-assisted cell printing does not cause any thermal cell injury due to very short exposure time of cells to laser pulses. Meanwhile, chemical cell injury is caused by usage of chemicals including calcium chloride solution. Mechanical, thermal, or chemical cell injuries cause biological damage to cells including protein damage, DNA damage, plasma membrane damage, loss of calcium ion homeostasis, accumulation of oxygen-derived free radicals, or metabolic energy (ATP) depletion. An overview of mechanisms of process induced cell injury is outlined in this section.

4.2 Physical Cell Injury

4.2.1 Mechanical Cell Injury

Bubble cavitation and droplet impact onto receiving substrate produce mechanical stresses during laser-assisted cell printing. The laser plasma generates high pressure in

the bioink. The high pressure results in formation of a gas bubble with high internal energy, around the center of the direct written place. Because the inside pressure of the initial gas bubble is higher than that of the surrounding bioink, the wall of the bubble travels at supersonic speeds for few nanoseconds and at subsonic speeds for few picoseconds. The rapid growth of the bubble induces high pressure on the adjacent cells. When the bubble reaches its maximum expansion, it collapses due to huge pressure difference between inside and outside mediums. The adjacent fluid rushes into the cavity which causes significant mechanical stress on cells in the area.

Droplet impact with the receiving substrate is another key factor that produces mechanical stress and causes mechanical damage in cell direct writing. When the droplet impacts onto the substrate, the droplet is compressed and deformed continuously before collapse. Consequently pressure at the collision interface changes and a shock wave is generated. The compression of droplets leads to the formation of a jet from the contact edges between the droplet and impact surface and results in rapid collapse of the droplet which causes significant mechanical stress on cells.

4.2.2 Thermal Cell Injury

During laser-assisted cell printing laser pulses thermodynamically interact with living cells which may injure cells. Thermal cell injury is caused due to optical heating by laser pulses which results from two mechanisms, photothermal and photochemical mechanisms. Photothermal mechanism is one in which melting, evaporation, and ejection of bioink occurs due to accumulation of photon energy as there is not sufficient energy in

photons of visible and infrared radiation to dissociate chemical bonds. Photochemical mechanism is one in which photons have sufficient energy to break chemical bonds. In absence of photochemical mechanism, the photon energy is absorbed by cells and causes temperature rise which may injure cells.

4.2.3 Chemical Cell Injury

Calcium chloride solution is used as receiving substrate in laser-assisted cell printing to facilitate gelation of ejected cell-laded alginate droplets. Gelation occurs because of osmosis of calcium ions into alginate droplets. However, the osmosis of calcium ions into alginate droplets alters transmembrane chemical ion gradients for the cells. Cells require certain transmembrane ion gradients to function and the alteration of gradients could be harmful to cells. Calcium ions are universal second messenger among cells and regulate vital cellular functions such as cell cycle regulation, proliferation, differentiation, gene expression, and cell death [Bernardi2007, Giorgi2008]. Alterations in intracellular as well as extracellular calcium ion concentrations have been reported to result in diverse cellular responses ranging from cell proliferation to cell death [Lee1992, Martino2011, McGinnis1999, McNeil1998]. Nature of response depends on cell type, concentration of calcium ions, and time duration of exposure of cells to calcium ions [Lee1992, McGinnis1999, McNeil1998].

4.3 Biological Cell Injury

4.3.1 Protein Damage (Denaturation/Unfolding)

Proteins are building blocks of a cell and execute most of its functions. Proteins constitute majority of the dry weight (up to 60%) of a cell. A protein molecule is made from a long chain of amino acids. Each amino acid is linked to its neighboring amino acid through a covalent peptide bond. Hence, proteins are also known as polypeptides. Each type of protein has a unique amino acid sequence and there are several thousand types of proteins [Alberts2008]. Proteins have complex structures that are important to their function. Each structure has numerous levels including primary, secondary, tertiary, and quaternary.

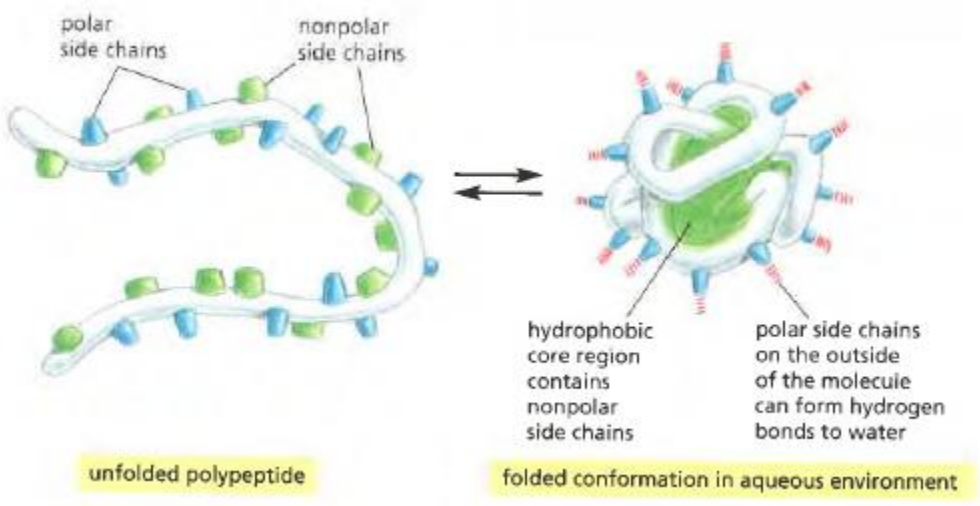

Figure 4.1: Protein folding into three dimensional functional structure [Alberts2008]

Proteins are initially synthesized as one dimensional ribbons in cells. Subsequently, the one dimensional ribbons acquire a functional three dimensional form

or a confirmation, one which minimizes their free energy [Alberts2008]. A protein is unable to carry out its specific function when its final confirmation is altered [Bischof2005]. The alteration of the protein final confirmation is called denaturation or unfolding. The protein unfolding is caused due to heat, cold, ionizing radiation, large transmembrane electrical potentials, reactive oxidation species, chemical agents, and external mechanical stresses [Agarwal2005].

Chaperons minimize the injury to the cells from protein damage by folding and refolding damaged proteins. There are two major types of chaperons, heat shock proteins (HSPs) and chaperonins. HSPs are expressed under conditions of cellular stress. HSPs bind tightly with unfolded or misfolded proteins and take them out of circulation. Chaperonins possess a cavity in which misfolded proteins are encapsulated and removed from circulation. When an injurious stress overwhelms the production of chaperons, unfolded proteins accumulate and form protein aggregates [Guo2005]. Such protein aggregation results in failure of vital cell functions and eventually causes cell death [Kampinga2006, Vos2008].

4.3.2 DNA Damage

Living cells store their hereditary information in DNA which is made from simple subunits called nucleotides [Alberts2008]. Each nucleotide consists of a sugar-phosphate molecule with a base attached to it. A base is a nitrogen-containing side group and there are four types of bases. They are adenine, guanine, cytosine, and thymine, corresponding to four distinct nucleotides labeled A, G, C, and T respectively. A normal DNA molecule consists of two complementary single strands [Alberts2008]. Each single strand of DNA

contains nucleotides joined together by sugar-phosphate linkages. The nucleotides within each strand are linked by strong covalent chemical bonds while the complementary nucleotides on opposite strands are held together by weak hydrogen bonds [Alberts2008]. The two strands twist around each other to form a double helix, a robust structure that can accommodate any sequence of nucleotides without altering its basic structure [Alberts2008].

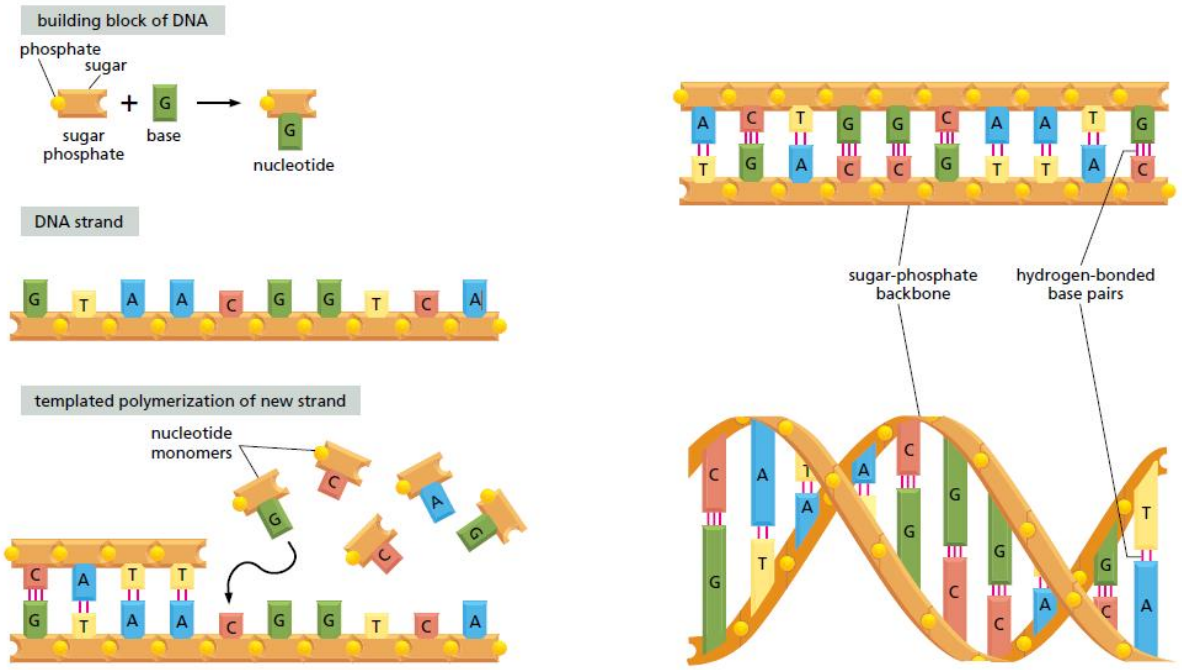

Figure 4.2: DNA building blocks [Alberts2008]

The genetic information in DNA primarily comprises of instructions for making proteins. Proteins are the macromolecules that execute the vital cell functions [Alberts2008]. Thus, DNA damage results in genetic mutation followed by protein malfunction, failure of vital cell functions, and eventually cell death. DNA damage can be caused by heat, spontaneous metabolic events, spontaneous base loss, ultraviolet

radiation, ionizing radiation, reactive oxidation species, environmental chemicals, and external mechanical stresses [Kao2005].

4.3.3 Plasma Membrane Damage

Cell membrane or the plasma membrane is the barrier that separates the cell interior from the exterior, chemically as well as electrically [Gissel2011]. A cell membrane primarily consists of lipid molecules that are arranged as a continuous double layer about 5 nm thick [Alberts2008]. The plasma membrane also contains protein sensors and ion channels. The receptors transfer information across the membrane through chemical signaling [Alberts2008]. Whereas, the ion channels control the transport of specific ions such as Na^{+}, K^{+}, $Ca^{2+,}$ and Cl^{-} across the membrane [Gissel2011].

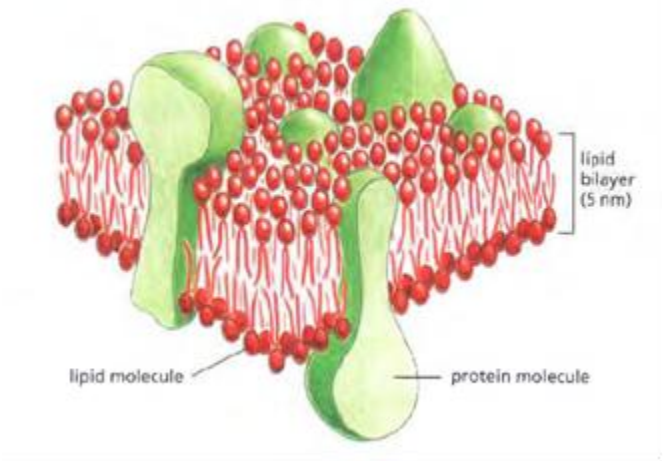

Figure 4.3: Three dimensional view of plasma membrane [Alberts2008]

Ion channels together with ion pumps and exchangers enable the cells to build up chemical and electrical gradients required for performing essential cellular functions.

Much of a cell's metabolic energy, used in the form of ATP catalysis, is consumed in maintaining such transmembrane gradients [Gissel2011]. The loss of plasma membrane integrity results in large influx of ions such as calcium ($Ca^{2+)}$ ions owing to very large transmembrane ion gradients.

The influx of calcium ions traumatizes the mitochondria of the cells and results in generation of reactive oxygen species. The oxygen free radicals further breakdown the plasma membrane and causes further influx of calcium ions [Gissel2005, Bernardi2007, Henriquez2008]. As the injured cells attempt to reverse the calcium ion overload, much of their metabolic energy is consumed in activating the transmembrane ion channels and pumps. The metabolic energy depletion results in influx of water into the cells owing to compromised energy dependent regulatory volume decrease (RVD) response which leads to increase in cell volume [Henriquez2008]. Such an increase in cell volume results in rupture of plasma membrane and eventually cell death [Henriquez2008].

4.3.4 Loss of Calcium Ion (Ca^{2+}) Homeostasis

Calcium ions are universal second messenger in cells and regulate vital cellular functions such as secretion, metabolic control, cell cycle regulation, cell proliferation, gene expression, and cell death [Bernardi2007, Giorgi2008]. Second messengers are the small intracellular signaling molecules, which amplify and relay the signals received at the receptors on the cell surface, to the target molecules in interiors of the cell [Alberts2008]. A variation in intracellular or extracellular calcium ion concentrations is harmful to cells as it affects transmembrane ion gradients [Giorgi2008]. The intracellular

calcium ion overload due to plasma membrane damage triggers the so called vicious cycle as shown in Figure 4.4 which eventually causes cell death [Gissel2005].

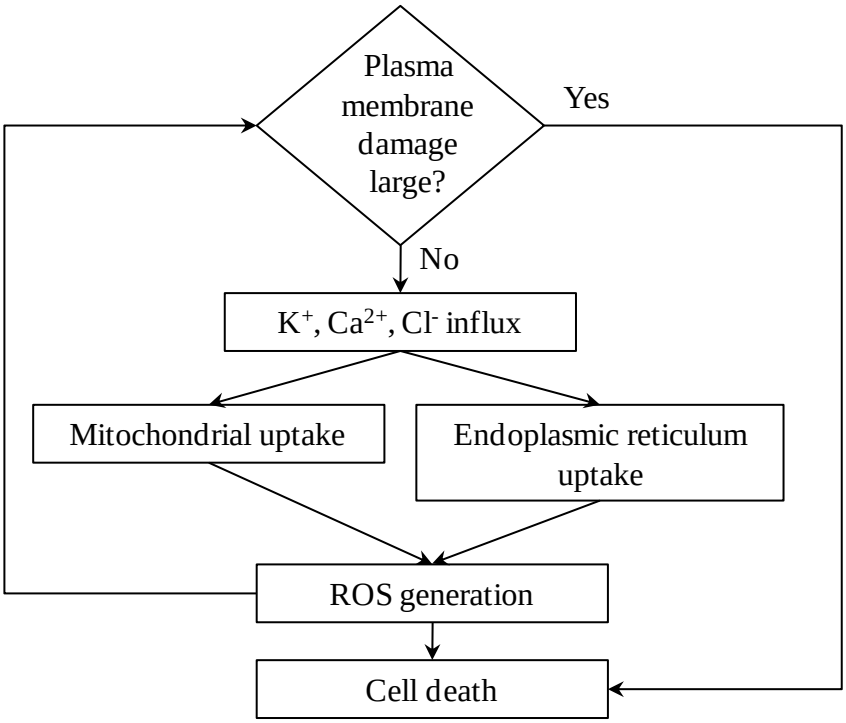

Figure 4.4: Calcium ion (Ca^{2+}) vicious cycle [Gissel2005]

4.3.5 Accumulation of Oxygen-derived Free Radicals

Cells generate energy by reducing molecular oxygen to water. During this process, cells generate oxygen free radicals as unavoidable by product of the mitochondrial respiration. These oxygen derived free radicals are termed as reactive oxygen species (ROS) [Kumar2005]. ROS play an important role in cell signaling, gene expression, cell proliferation, and cell death in healthy cells [Henriquez2008]. ROS are kept in check by antioxidants.

However, when cells are exposed to ultraviolet rays, radiation, toxic chemicals, and mechanical stresses, the balance between ROS and antioxidants is disturbed. As a

result, ROS accumulate in cells and oxidize essential organelles such as lipids (cell membrane), proteins, and DNA. This in turn compromises vital cell functions which eventually causes cell death.

4.3.6 Metabolic Energy (ATP) Depletion

Adenosine triphosphate (ATP) carries chemical energy within cells for metabolism. ATP is required for vital cell functions such as cell injury repair, membrane transport, protein synthesis, motility, and cell division [Kumar2005]. ATP is produced in two ways. The first is oxidative phosphorylation of adenosine diphosphate in presence of oxygen in mitochondria. The second is ATP generation in absence of oxygen using glucose derived from body fluids or hydrolysis of glycogen [Kumar2005]. ATP depletion reduces plasma membrane ion pumps activity which disrupts the transmembrane gradients. Due to this vital cellular functions are disrupted. Furthermore, in cells deprived of ATP, proteins may become misfolded and can result in cell death.

4.4 Modes of Cell Death

Cell injury is reversible up to a limit. However, beyond the limit, cell injury is irreversible and cell suffers cell death [Kumar2005]. Cell death is of two types, programmed cell death and accidental cell death. Programmed cell death is identical to death by suicide (controlled building implosion). In contrast, accidental cell death is similar to death by murder (uncontrolled building explosion) [Majno1995].

Programmed cell death is a process by which the cell commits suicide when malfunctions arise from cell stress, cell injury, or conflicting cell division signals

[Fussenegger2000]. Programmed cell death is mediated by an intracellular genetic death program to eliminate unwanted, harmful, or cells that outlived their usefulness [Kulka2006]. Cells undergoing programmed cell death go through an ordered series of morphological changes which require RNA and protein synthesis [Baehrecke2011].

4.4.1 Apoptosis

Apoptosis is a programmed cell death which is characterized by reduction of cellular volume (pyknosis). The cell undergoes nuclear and chromatin condensation in initial stages. Later, plasma membrane experiences blebbing or irregular bulging. Afterwards, the cell breaks up into plasma membrane enclosed fragments known as apoptotic bodies. Finally, apoptotic fragments are recognized and engulfed by neighboring cells. Plasma membrane remains intact until final stages of apoptosis. However, its structure is altered to enable engulfment by neighboring cells. Apoptosis does not result inflammatory reaction as dead cells are removed before their contents are released. Failure of apoptosis is often associated with development and progression of cancer [Kroemer2009].

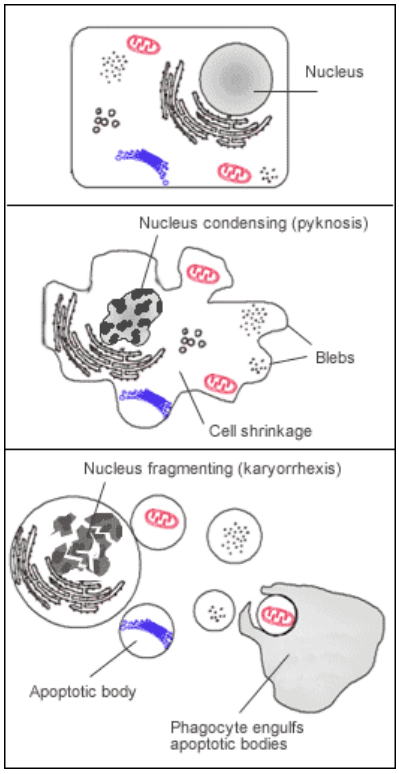

Figure 4.5: Apoptotic cell death

Caspases are enzymes that degrade proteins. Caspases trigger and execute apoptosis which are comparable to dynamite employed during controlled implosion of buildings. There are two types of apoptotic caspases, initiator and effector caspases. Initiator caspases activate effector caspases which in turn activate various other proteins within the cell to trigger apoptosis. The cascade of caspases is regulated by caspase inhibitors. The inhibitors bind to caspases and block their functions, until the inhibitors are completely saturated with caspases.

Extrinsic Pathway

Apoptosis is initiated through two major pathways, at the plasma membrane by death receptor ligation (receptor pathway) or at the mitochondria (mitochondrial pathway) [Fulda2006]. The extrinsic pathway is activated when a proapoptotic ligand such as CD95 ligand (CD95-L) or TRAIL binds to specialized proapoptotic membrane receptors such as death receptors of the tumor necrosis factor (TNF) receptor or TNF-related apoptosis-inducing ligand (TRAIL) receptors [Ashkenazi2002, Fulda2006]. Ligands are signaling molecules released by other cells such as natural killer (NK) cells of human immune system [Csipo1998].

Initially in extrinsic pathway, soluble molecules belonging to Tumor Necrosis Factor (TNF) family bind to receptors (TNF-R) on plasma membrane. TNF-R possess a Death Domain (DD) which recruits other Death Domain containing proteins such as TNF-R type 1-Associated Death Domain protein (TRADD) and Fas-Associated protein with Death Domain (FADD). TRADD and FADD bind to inactive caspases-8 and -10 (procaspases-8 and -10) and activate them [Zhang2009].

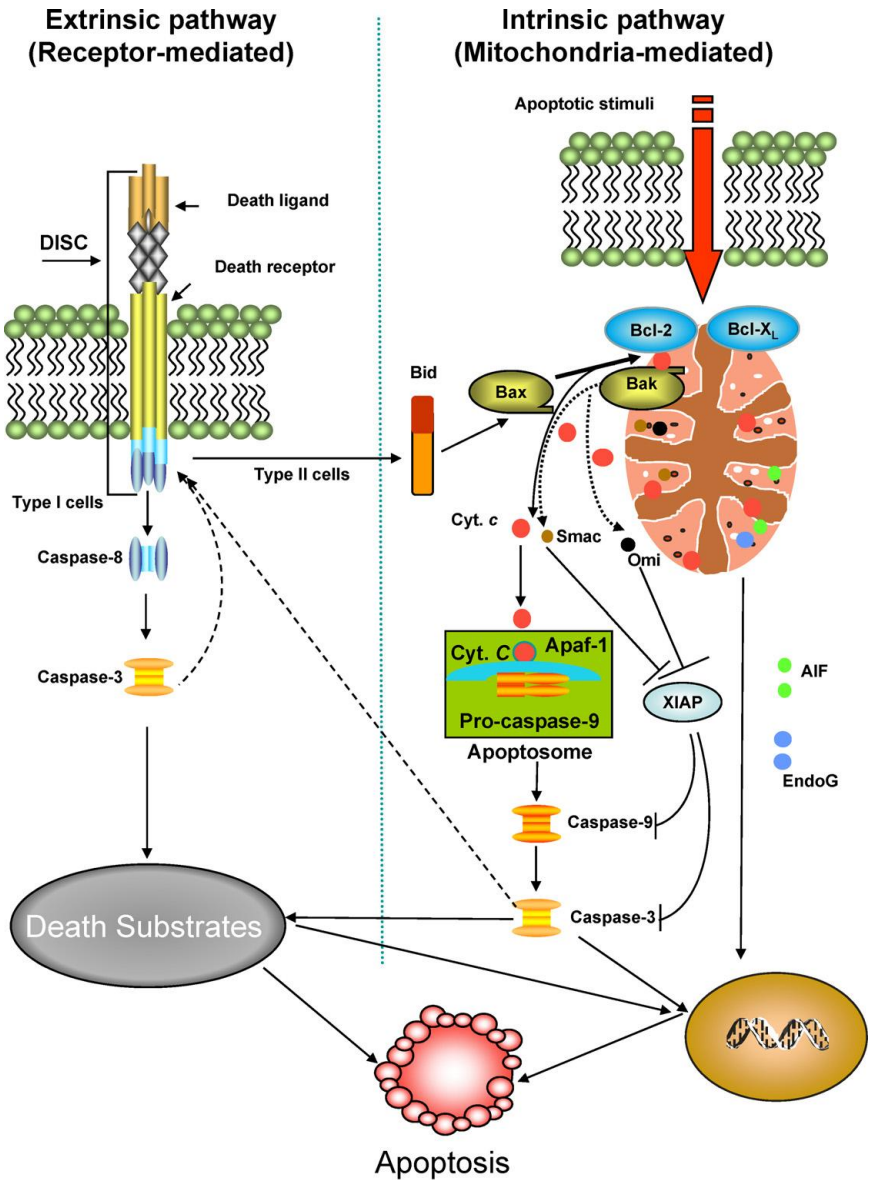

Figure 4.6: Apoptosis extrinsic and intrinsic pathways [Zhivotovsky2011]

The complex formed by TRADD, FADD, caspase-8, and caspase-10 is referred as Death Inducing Signaling Complex (DISC). Active caspases-8 and -10 in turn activate inactive effector caspases -3, -6, and -7. Active effector caspases -3, -6, and -7 executes cellular dismantling [Zhang2009, Giansanti2011]. In some specific cells, known as type I

cells, caspase-8 is produced in sufficient quantities to activate inactive caspase-3. However, in some specific cells, known as type II cells, caspase-8 is not produced in sufficient quantities to activate inactive caspase-3. In such cells, caspase-3 activation requires amplification through intrinsic pathway [Bagci2006].

Intrinsic Pathway

The intrinsic pathway or mitochondrial pathway is activated in response to various harmful intrinsic stresses such as DNA damage, protein damage, oxidative stress, loss of ion homeostatic control, oxygen deprivation (hypoxia), and growth factor deprivation. The hallmarks of intrinsic pathway are increased mitochondrial permeability and subsequent release of pro-apoptotic molecules into the cytoplasm. Pro-apoptotic BH3 proteins are activated initially in response to intrinsic stress. However, BCL2 inhibitory proteins bind to BH3 proteins and block them. Sustained intrinsic stress activates additional BH3 molecules and saturates BCL2 molecules. Free BH3 molecules induce conformational changes in BAX molecules and translocate them to mitochondria outer membrane [Zhang2009].

BAXm, the mitochondria membrane localized BAX molecules, increase mitochondrial outer membrane permeability (MOMP). Consequently, pro-apoptotic molecules such as Cytochrome complex (CytoC), SMAC, and apoptosis-inducing factor (AIF) escape into cytoplasm from mitochondria. Later, CytoC activates caspase-9 while SMAC inhibits XIAP, an inhibitor of caspase-3. Next, caspase-9 activates caspase-3. Active caspase 3 together with other executioner caspases activates various protein substrates which culminate apoptosis [Zhang2009].

4.4.2 Necrosis

Necrosis is an accidental cell death which involves rapid swelling of the cell, membrane rupture, and subsequent release of cell contents as a consequence of overwhelming physical (membrane damage, loss of ion homeostasis) or chemical (toxicity, ATP depletion) trauma to the cell. The cell death due to necrosis is a passive consequence of irreparable damage as opposed to active choice of the cell in programmed cell death [Henriquez2008]. For many years, necrosis has been synonymous with accidental cell death. However, new evidence suggests that necrosis, like apoptosis, can be executed by regulated mechanisms under certain circumstances [Hitomi2008, Galluzzi2008].

4.5 Process-induced Cell Injury Mechanisms in Laser-assisted Cell Printing

During laser-assisted cell printing, the process-induced cell injury and cell death are mainly due to the mechanical stresses, gel membrane thickness, and calcium ion diffusion. The mechanical damage can be observed immediately and is controlled by the laser fluence, while the biochemical damage can be detected after gelation and/or incubation and is controlled by the gel membrane thickness and calcium ion diffusion.

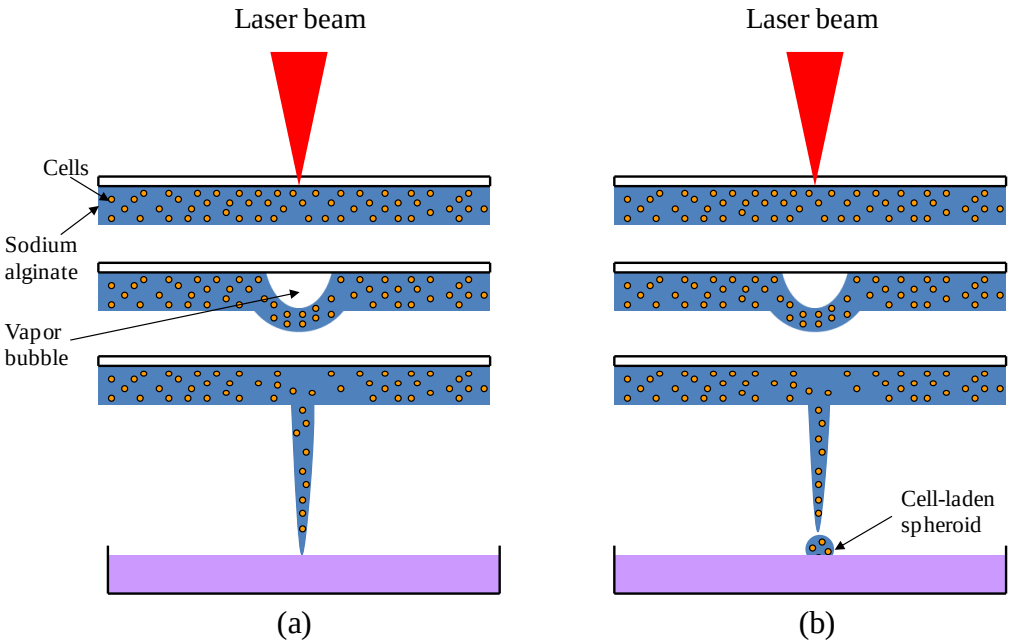

Figure 4.7: Two possible schematics of laser-assisted cell printing process. (a) jet-based printing; (b) droplet-based printing

The mechanical stresses are generated during jet/droplet formation and landing [Barron2004c, Hopp2005b], as can be seen in Figure 4.7, which illustrates the whole printing process. The bioink is subjected to acceleration during jet/droplet formation process, while subjected to deceleration during jet/droplet landing process. These mechanical stresses could break the cell plasma membrane, resulting in necrosis or trivial injury of cells, depending on the severity of damage suffered by the cells. The mechanical stresses could also induce apoptosis of the cells, by generating moderate cell injury, damaging DNA, organelle, etc [Mayr2002].

Irreversible protein damage occurs when a protein temperature exceeds 45 °C [Bischof05] whereas irreversible DNA damage occurs when the DNA temperature exceeds 85 – 90 °C [Bischof2005]. Meanwhile, at temperatures above 43 °C, the kinetic energy of the lipid bilayer molecules exceeds hydration energy barrier and results in

mechanical disruption of the plasma membrane [Orgill2005]. It has been demonstrated that UV radiation and heat have negligible effect on post-transfer cell viability in laser-assisted cell printing [Lin2009b] [Ringeisen2004].

Gelation process also effect on post-transfer cell injury and cell viability. Figure 4.8 shows the schematic of gelation process, including partial gelation (about 2 minutes) and complete gelation (about 3-4 minutes) [Blandino1999]. Alginate molecules are cross-linked by calcium ions when exposed to $CaCl_2$ solution. The gelation process goes towards the center of the sphere. On one hand, the formation of gel, especially a thick gel membrane, can block the oxygen or nutrition influx, which may cause injury to cells. On the other hand, the calcium ion diffusion also contributes to cell injury when encapsulated cells are exposed to calcium ions. This is because the overload of calcium ions results in generation of reactive oxygen species (ROS) [Gissel2005, Bernardi2007], which causes membrane lipid peroxidation, cross-linking and degradation of proteins, and nicking of DNA, and then apoptosis occurs due to these factors [Harsdorf1999] [Simon2000]. ROS generation further breaks down the plasma membrane and causes further influx of calcium ions into the cells triggering the so called calcium ion vicious cycle [Gissel2005, Bernardi2007, Henriquez2008]. Calcium ions can be injurious to cells since cells require certain transmembrane ion gradients for their survival [Gissel2005, Bernardi2007, Giorgi2008] and the osmosis of calcium ions into the alginate droplets alters the transmembrane calcium ion gradient for the encapsulated cells [Campanella2004]. The diffusivity of calcium ions can be characterized by the combined diffusion coefficient

Dm, which is defined as the combination of the diffusivity of the microcapsule membrane and the diffusivity of the core solution,

$$D_m = \frac{r_b}{\frac{r_b - r_a}{D_1} + \frac{r_a}{D_2}} \qquad (4.1)$$

where D1 and D2 are diffusion coefficients of gel membrane and core solution respectively, and ra and rb are the internal radius and external radius of the microcapsule respectively. A larger Dm indicates a larger diffusivity [Chai2004].

In this study, post-transfer cell injury repair is assumed based on the observation that control cell population remained constant from 0 to 24 hours, indicating no cell proliferation during the first 24 hours of incubation.

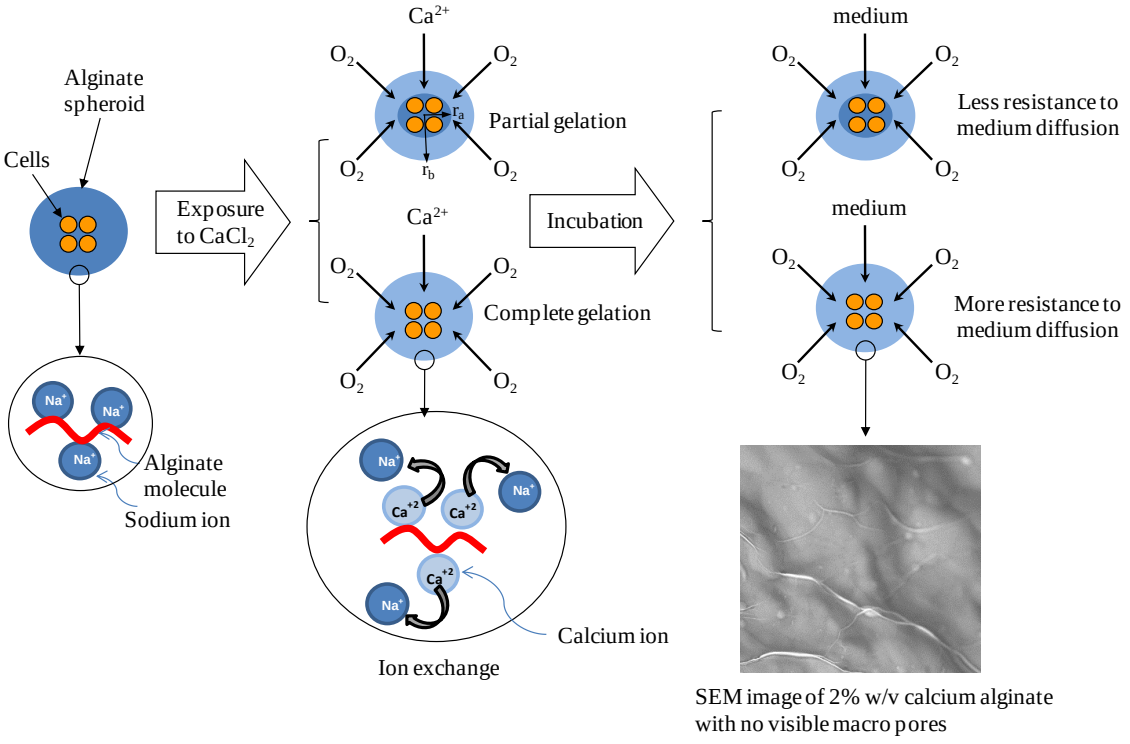

Figure 4.8: Alginate gelation schematic with respect to gelation time over 24 hours of incubation

4.6 Summary

Process-induced cell injury in laser-assisted cell printing is of three types, mechanical cell injury, thermal cell injury, and chemical cell injury. Process-induced cell injury arises because of biological damage to cells including protein damage, DNA damage, plasma membrane damage, loss of calcium ion homeostasis, accumulation of oxygen-derived free radicals, or metabolic energy (ATP) depletion. Process-induced cell injury is reversible up to a certain limit. However, beyond the limit the injury becomes irreversible and cell death occurs through either apoptosis or necrosis.

CHAPTER FIVE

RESULTS AND DISCUSSION

5.1 Introduction

The effects of alginate gelation, gelation time, alginate concentration, and the effect of operating conditions such as the laser fluence on post-transfer cell viability during laser-assisted cell printing are studied herein. Post-transfer cell viability is measured both immediately after printing and after 24 hours of incubation. However, the latter is of more interest than the former since the injured cells require time to complete cell injury repair and completion of apoptosis may take several hours. Therefore, post-transfer cell injury and cell viability after 24 hours of incubation are emphasized in this study, and the ones for immediately after printing are for comparison only.

5.2 Observations after 24 hours of Incubation and Discussion

5.2.1 Effect of gelation

Experimental results of Experimental setup A are shown in Figure 5.1. It can be seen that comparing with the no gelation condition (printing cells into DMEM), two-minute gelation increased cell viability while ten-minute gelation decreased cell viability for all laser fluences. Moreover, for no gelation condition, cell viability decreased after 24 hours of incubation for all laser fluences. For two-minute gelation condition, cell viability increased at both 800 and 1200 mJ/cm^2 laser fluences after 24 hours of incubation but decreased at 1600 mJ/cm^2 laser fluence. However, for ten-minute gelation

condition, cell viability only increased at 800 mJ/cm^2 laser fluence after 24 hours of incubation, and decreased at both 1200 and 1600 mJ/cm^2 laser fluences.

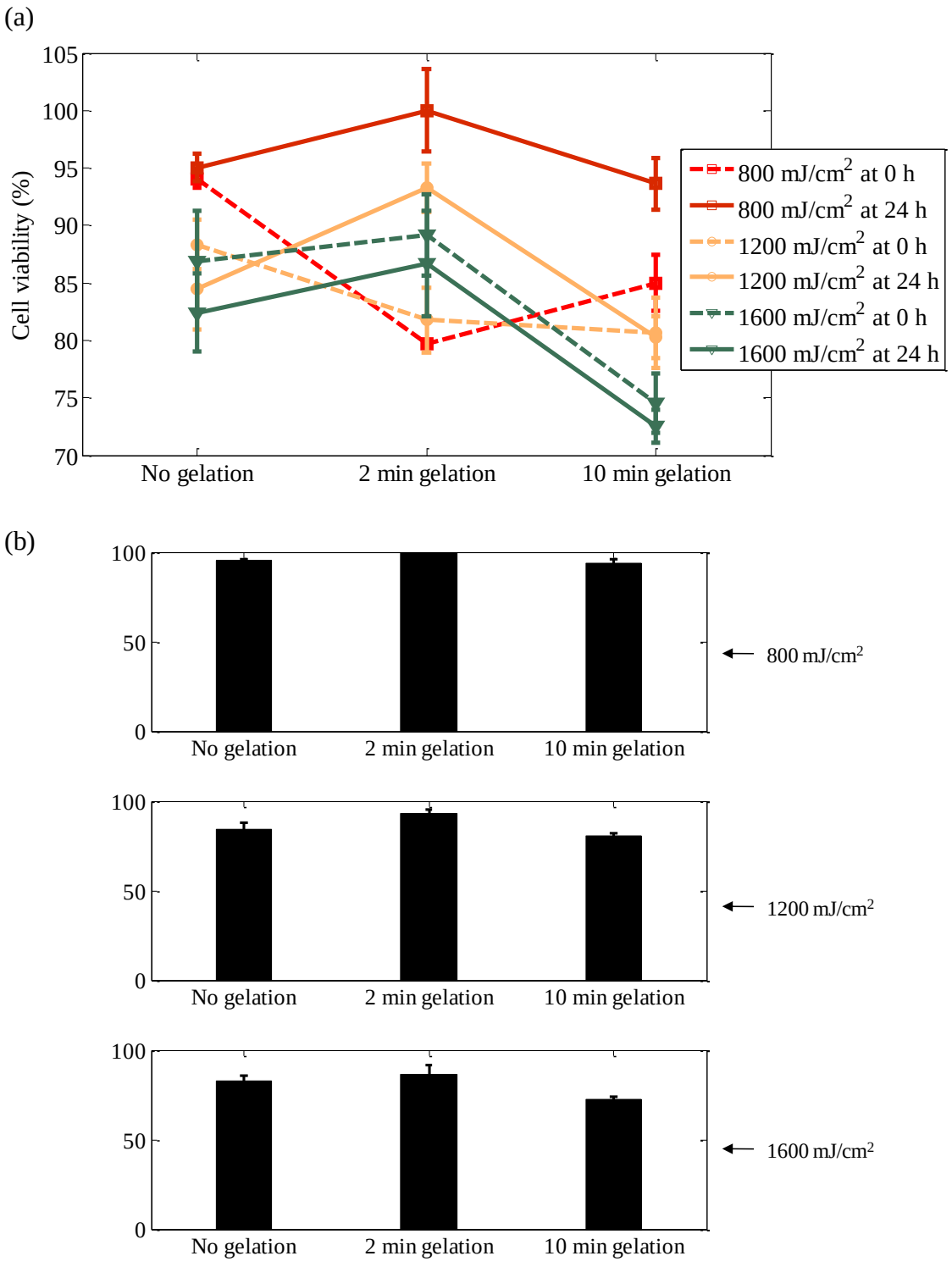

Figure 5.1: Effect of gelation on cell viability in relation with laser fluence. (a) immediately and after 24 hours; (b) after 24 hours

After 24 hours of incubation, cell viability for two-minute gelation condition is higher than that of no gelation condition because of cushion effect by forming gel membrane during droplet impact. That is, for two-minute gelation condition, forming gel membrane during alginate droplet impact has minimized mechanical stresses. However, for no gelation case, alginate droplets have lacked the gel membrane during droplet impact to minimize the mechanical stresses. Cell viability for ten-minute gelation condition is lower than that of no gelation condition after 24 hours. This is because the droplets have been completely gelled for ten-minute gelation condition. Complete gelation of droplet occurs during 3-4 minutes of alginate droplet interaction with calcium chloride [Blandino1999]. Thus, diffusion of oxygen and nutrients from culture medium into completely gelled droplets was limited (Figure 4.8) because of the thick gel membrane during 24 hours incubation. As a result, encapsulated cells, especially injured cells, died because of nutrient deprivation [Agarwal2005, Kumar2005].

For no gelation condition, cell viability decreased after 24 hours of incubation at all laser fluences. This indicates that more injured cells suffered irreversible cell injury than reversible cell injury and died because of apoptosis. The apoptotic cells were initially viewed under microscope as bright and colorless when stained with trypan blue assay because of their intact plasma membrane. However, after 24 hours of incubation, plasma membrane of late apoptotic cells was compromised and the cells were viewed as blue/dead. At the same time, cells which had suffered reversible cell injury (trivial plasma membrane damage) were initially viewed as blue but became bright and colorless

after 24 hours of incubation since they were repaired (plasma membrane resealed). Therefore, the decreasing trends could be seen.

Cell viability for two-minute gelation condition increased after 24 hours of incubation at laser fluences of 800 and 1200 mJ/cm^2. This indicates that during the 24 hours of incubation, injured cells were able to repair the injury, including resealing their plasma membrane and restoring their intra cellular Ca^{2+} concentration to normal levels. However, the cell viability decreased at laser fluence of 1600 mJ/cm^2. This is because more cells suffered irreversible cell injury and died because of apoptosis than reversible cell injury at 1600 mJ/cm^2. The apoptotic threshold increased for cells subjected to two-minute gelation because of the cushion effect of gel membrane and more energy was needed to induce apoptosis.

Cell viability for ten-minute gelation condition increased after 24 hours of incubation at 800 mJ/cm^2 laser fluence, while decreased at 1200 and 1600 mJ/cm^2 laser fluences. The reason for the decrease of cell viability at 1600 mJ/cm^2 laser fluence and the increase of cell viability at 800 mJ/cm^2 laser fluence are similar to the two-minute gelation case. However, cell viability decreased slightly at laser fluence of 1200 mJ/cm^2 after 24 hours of incubation. This indicates that the microsphere gel membrane thickness played a more important role in cell injury, and this can be also seen in Figure 4.8 for two- minute and ten-minute gelation conditions. Actually, the injured cell recoverability was lower for ten-minute gelation condition than two-minute gelation condition. This is because of greater magnitude of injury (Ca^{2+} induced cell injury) suffered by cells owing to longer exposure time of encapsulated cells to calcium chloride and also because of

limited nutrient transport to encapsulated cells during 24 hours incubation owing to thick gel membrane.

5.2.2 Effect of Laser Fluence

(a)

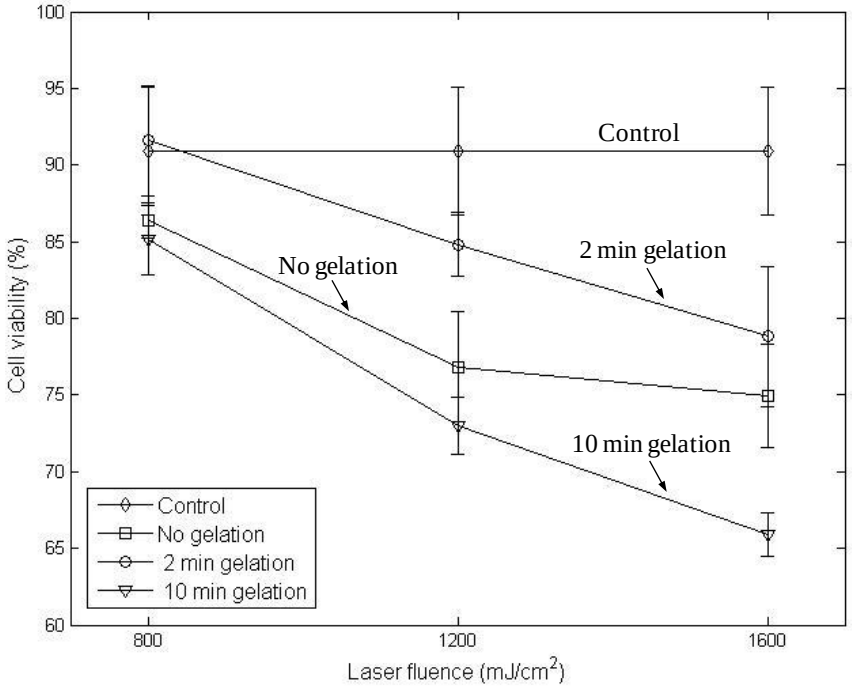

(b)

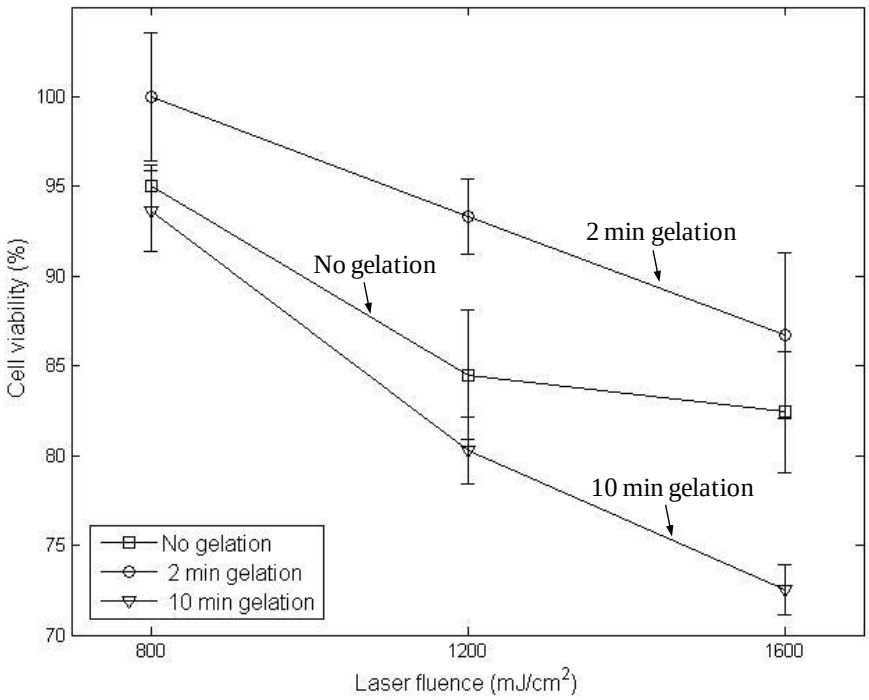

Figure 5.2: Effect of laser fluence on cell viability after 24 hours of incubation. (a) control effect is not considered; (b) control effect is considered

Experimental results of Experimental setup A are shown as curve graphs in Figure 5.2, which illustrates the relationship between the post-transfer cell viability and the applied laser fluence after 24 hours of incubation. It can be seen from Figure 5.2 that the post-transfer cell viability decreases with increase in laser fluence for all these three cases. This relationship is the result of the process-induced mechanical stress, including jet/droplet formation and landing, and the calcium ion diffusion due to the microsphere size.

For the cells subjected to no gelation, it has been demonstrated that the jet/droplet formation acceleration is higher, and that the jet/droplet landing deceleration is higher at higher laser fluence, generating larger normal/shear stress, resulting in a lower cell viability [Wang2008, Lin2009b, Lin2010]. For two-minute gelation and ten-minute gelation conditions, gel membrane forms immediately when the jet/droplet contacts the calcium chloride solution inside the substrate container, minimizing the impact of the normal/shear stress of landing process on cell viability [Ringeisen04]. Thus, the landing-induced cell injury did not have much influence on cell viability for cells subjected to gelation. Therefore, cell injury is only related with jet/droplet formation process. The mechanical stress generated during the jet/droplet formation process increases with laser fluence which decreases cell viability.

The calcium ion diffusion also contributes to cell injury when encapsulated cells are exposed to calcium ions. As can be seen from Equation 4.1, the increase in laser fluence results in the increase of droplet/microsphere diameter (r_a and r_b) [Duocastella2009], whereas the membrane thickness remains constant, such that (r_b-r_a) is

constant. Hereby, the increase of laser fluence decreases the combined diffusion coefficient (D_m) [Chai2004]. Thus, the cells are exposed to less calcium ions, which increases the cell viability.

Therefore, the decreasing cell viability with laser fluence is the combining effects of the mechanical stress generated during the jet/droplet formation process and the calcium ion diffusion, which is different from cells subjected to no gelation. Moreover, the mechanical stress played a more important role than calcium ion diffusion on cell injury. As a result, cell viability decreased with laser fluence for cells subjected to gelation.

5.2.3 Effect of Alginate Concentration

Experimental results of Experimental setup B are shown in Figure 5.3, which illustrates the relationship between the post-transfer cell viabilities and the sodium alginate concentration with cells subjected to no gelation as well as two-minute gelation after 24 hours of incubation. The sodium alginate concentrations used are 1%, 2% and 3%. It can be seen from Figure 5.3 that generally, the cell viability for both cases decreases with increase insodium alginate concentration. This trend is mainly attributed to the competing effect of process-induced mechanical stresses.

(a)

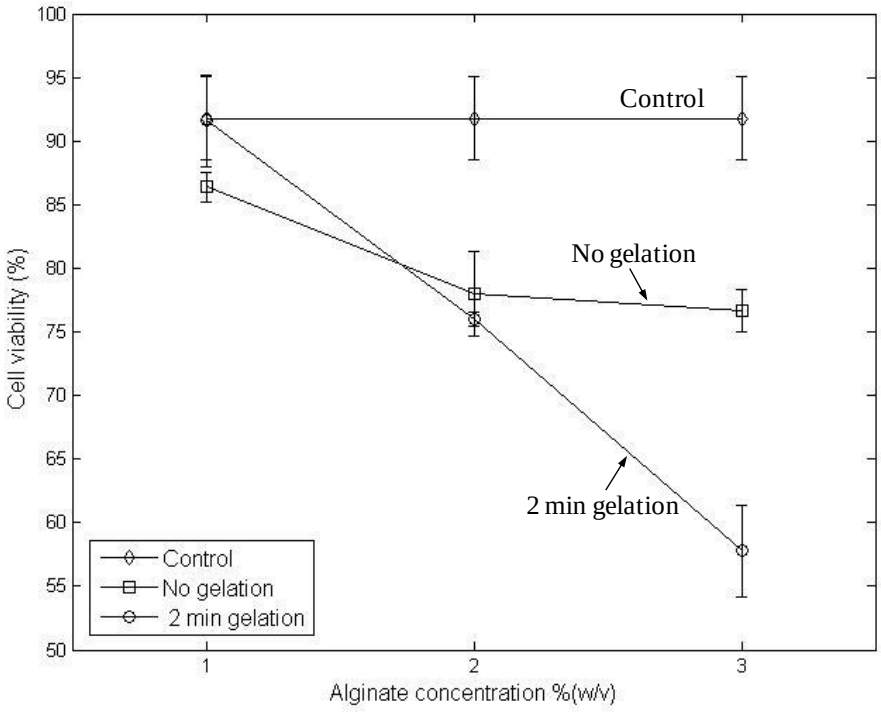

(b)

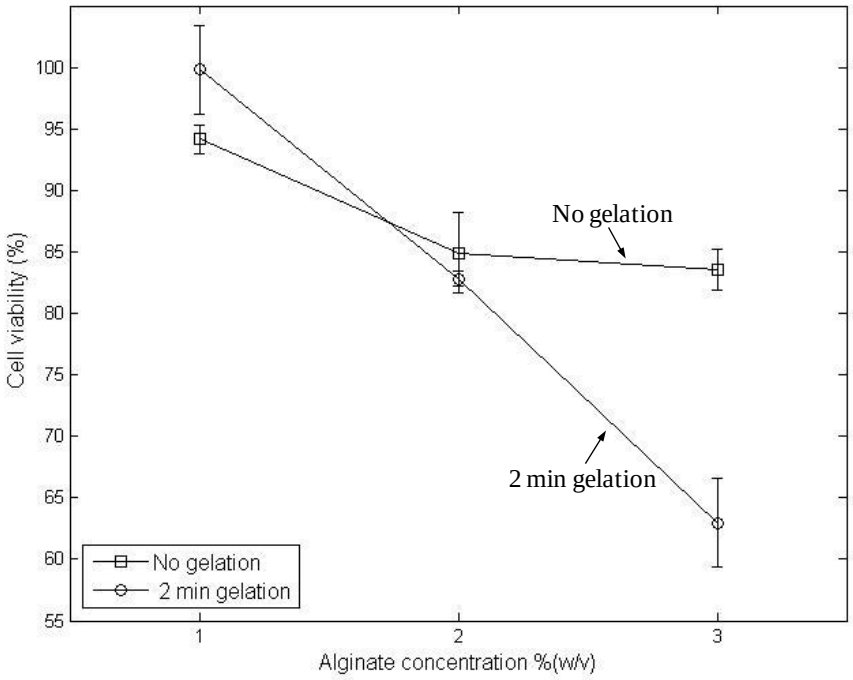

Figure 5.3: Effect of sodium alginate concentration on cell viability at steady state. (a) control effect is not considered; (b) control effect is considered

First, the viscosity of sodium alginate solution increases with sodium alginate concentration [Khalil2006, Gruene2011D, Lin2009a], which concerns with the mechanical stresses. On one hand, the stress generated during the jet/droplet formation process increases due to more stretches in polymer chains with higher sodium alginate concentration, which could decrease the cell viability. On other hand, both the acceleration and deceleration during the jet/droplet formation and landing process decreasesdue to increase in bioink viscosity, which could increase the cell viability.

Second, for the cells subjected to gelation, an increase in sodium alginate concentration results in a smaller microsphere with thinner gel membrane, which increases combined diffusion coefficient (D_m) [Lin2011] [Chai2004]. At the same time, an increase in sodium alginate concentration will also results in a more dense gel structure, which decreases D_m [Chai04]. The two factors also compete with each other [Chai2004]. However, the diameter of the microsphere decreases only less than 5% when sodium alginate concentration increases from 2% to 3% [Lin2011], which has not much influence on both the combined diffusion coefficient (D_m) and gel structure.

Hereby, the effect of sodium alginate concentration on combined diffusion coefficient is considered less significant in this study. Thus, even though pore diameter of the gelled alginate microspheres decreases with sodium alginate concentration [Yao2012], it does not have much influence on cell viability for either calcium ion influx or nutrition influx when encapsulated cells are exposed to calcium chloride solution (after printing) or DMEM medium (during incubation). In summary, the decreasing trend of

post-transfer cell viabilities for cells subjected to either gelation or no gelation is due to the competing effect of process-induced mechanical stresses.

5.3 Observations Immediately after Printing and Discussion

5.3.1 Effect of Gelation

The effect of gelation on post-transfer cell injury and cell viability is also studied immediately after printing/gelation for comparison. Experimental results of Experimental setup A are shown as bar graphs in Figure 5.4. At 800 mJ/cm^2 and 1200 mJ/cm^2 laser fluences, cell viability for two-minute gelation is lower than ten-minute gelation, while at 1600 mJ/cm^2 laser fluence, cell viability for two-minute gelation is higher than ten-minute gelation. These trends are a complex combining effects since cells immediately after printing require time to complete cell injury repair or to execute apoptotic cell death.

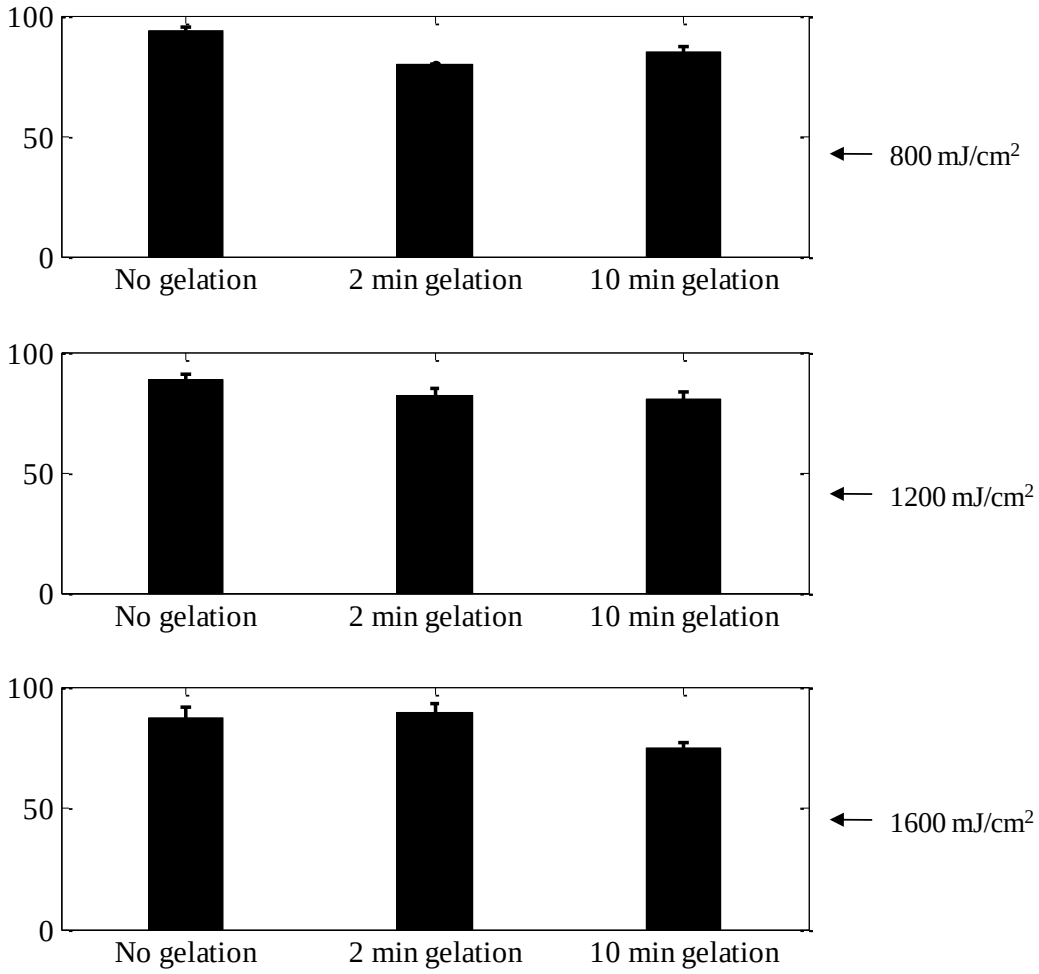

Figure 5.4: Effect of gelation on cell viability in relation with laser fluence immediately after printing/gelation

However, it can be seen that generally both two-minute gelation and ten-minute gelation decrease cell viability. Alginate jet/droplet undergoes gelation during the impact with receiving substrate, which is calcium chloride solution. The gelation occurs because of the osmosis of calcium ions into the alginate microspheres [Cao2012] as shown in Figure 4.8. Cells require certain transmembrane ion gradients for their survival

[Gissel2005, Bernardi2007, Giorgi2008]. In eukaryotic cells, intracellular (cytosolic) Ca^{2+} is maintained approximately at 100 nM while the extracellular Ca^{2+} is nearly 1 mM [Orrenius2003, Rizzuto2006].

Increase in extracellular Ca^{2+} has been reported to promote differentiation while inhibiting proliferation in mice epidermal cells (1.2 mM Ca^{2+}) and human breast epithelial cells (1.05 mM Ca^{2+}) [Hennings1980, Ochieng1991]. Meanwhile, Higher proliferation rates have been reported for rat fibroblast cells when extracellular Ca^{2+} is increased to 2 mM for 24hours [McNeil1998]. Contrastingly, an increase in extracellular Ca^{2+} to 5mM for 24 hours has been reported cause death of SH-SY5Y human neuroblastoma cells [McGinnis1999]. Furthermore, hybridoma cell viability has been reported to decrease in mere few minutes (40 – 60 min) when extracellular Ca^{2+} was increased to 115-135 mM (1.3 – 1.5% w/v) [Lee1992]. Over all, a significantly large increase in extracellular Ca^{2+} concentration (1 – 2 % w/v CaCl2) results in a lower cell proliferation rate [Xu2013] and even cell death [Lee1992]. Thus, the osmosis of calcium ions into the alginate droplets during gelation is injurious to the encapsulated cells as it alters the transmembrane calcium ion gradient for the cells [Campanella2004].

5.3.2 Effect of Laser Fluence

In this section, the effect of laser fluence on post-transfer cell viability is investigated at different gelation times in addition to cells subjected to no gelation immediately after printing/gelation. It can be seen from Figure 5.5 that generally, post-transfer cell viability decreases with increase in laser fluence for no gelation and ten-minute gelation cases. At the same time, cell viability increased for two-minute gelation.

For no gelation condition, it has been demonstrated that the jet/droplet formation acceleration is higher, and that the jet/droplet landing deceleration is higher at higher laser fluence, generating higher normal/shear stress, resulting in lower cell viability [Wang2008, Lin2009b, Lin2010]. For two-minute gelation condition, cell viability appears to increase with increase in laser fluence. There are two competing effects at play when laser fluence increases for two minutes gelation condition. One is mechanical cell injury due to mechanical stresses generated during droplet formation and droplet impact increases with increase in laser fluence [Wang2008, Lin2009b, Lin2010]. The other is injury due to Ca^{2+} ions decreases with increase in laser fluence. This is because the droplet size increases with increase in laser fluence which decreases combined diffusion coefficient D_m according to Equation 4.1. Hence, at smaller laser fluences, more cells have suffered reversible cell injury due to Ca^{2+} ions while at larger laser fluences more cells have suffered irreversible cell injury due to mechanical stresses and had died due to apoptosis. Because apoptosis is not detectable by trypan blue assay immediadiately owing to intact plasma membrane, cell viability is appearing to increase for two minutes gelation condition.

For ten-minute gelation, cell viability decreases with increase in laser fluence. Though, the forming gel membrane minimizes mechanical stresses during droplet impact, the longer exposure of encapsulated cells to calcium chloride has resulted in greater cell injury due to Ca^{2+}. Hence, injured cells died because of necrosis than apoptosi. Because, necrosis is immediately detectable by trypan blue assay, cell viability for ten-minute gelation condition is decreasing with increase in laser fluence.

(a)

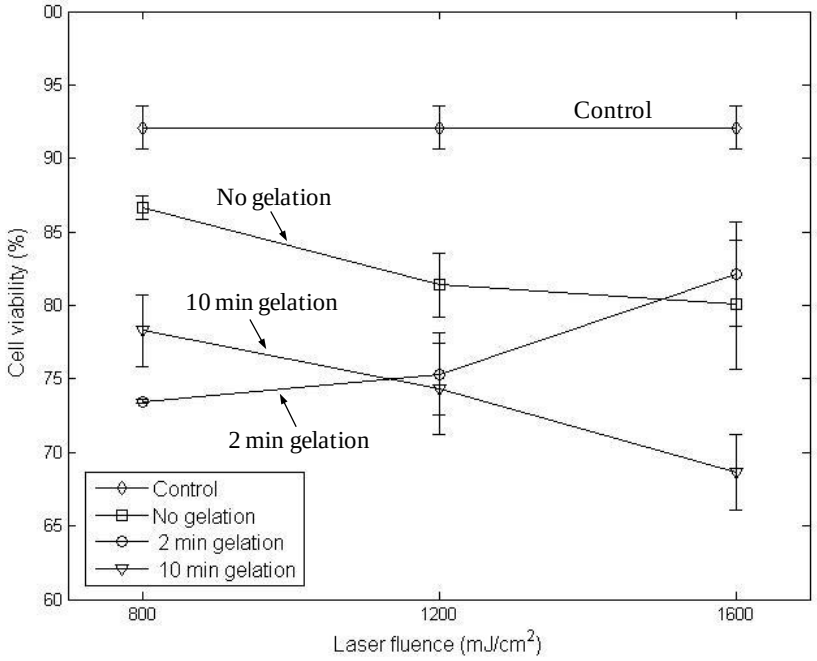

(b)

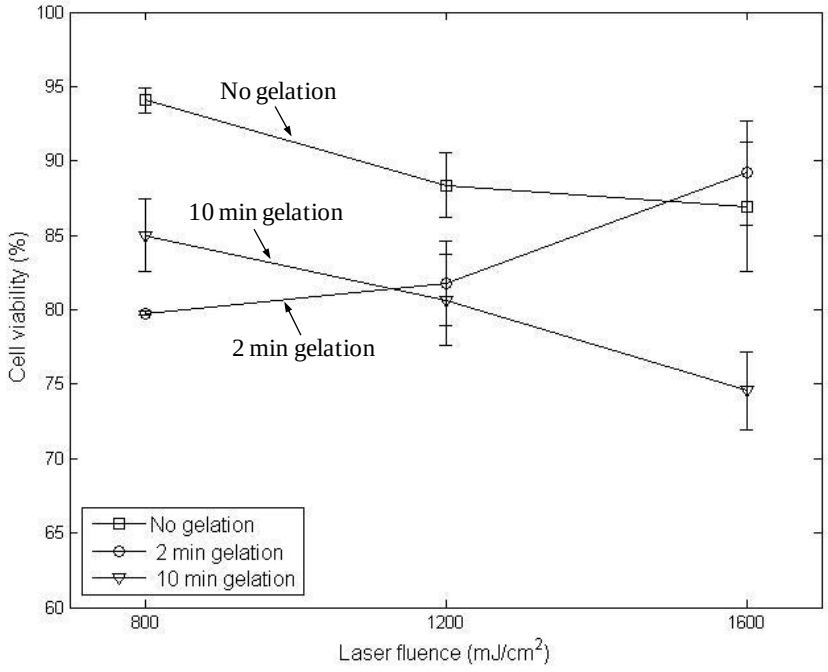

Figure 5.5: Effect of laser fluence on cell viability immediately after printing/gelation. (a) control effect is not considered; (b) control effect is considered

5.3.3 Effect of Alginate Concentration

The effect of sodium alginate concentration is not cared in this section since gelation needs time to complete and cells immediately after printing/gelation are unsteady. The gelation effect is also complex for cells immediately after printing and no regular trends can be found, and is not shown herein.

5.4 Statistical Analysis

Two-sample t-test was used for checking the following null hypotheses, two minutes gelation time does not improve the cell viability while ten minutes gelation time does not decrease the cell viability, of the encapsulated cells after 24 hours incubation. The two-sample t-test was performed on the following sets of cell viability data at a 95% confidence interval – no gelation and two minutes gelation, no gelation and ten minutes gelation, and two minutes gelation and ten minutes gelation. The p-value for each of the tests is less than 0.05 indicating significant statistical difference between each of the data sets. Hence, the null hypotheses were rejected.

5.5 Summary

Process-induced cell injury during alginate gelation in laser-assisted cell printing is systematically elucidated through investigating the effects of operating conditions and material properties on the post-transfer cell viability and cell injury reversibility. Two-minute gelation is observed to increase cell viability over 24 hours because of cushion effect. That is, forming gel membrane has minimized mechanical stresses generated during droplet impact. Despite ten minutes gelation having a cushion effect during

droplet landing, it is observed to decrease cell viability over 24 hours because of the thick gel membrane which reduces nutrient diffusion from culture medium. Also, the longer exposure of encapsulated cells to calcium chloride has resulted in greater cell injury due to Ca^{2+} ions. Increase in laser fluence as well as alginate concentration is found to decrease cell viability by introducing greater mechanical stresses during droplet formation.

CHAPTER SIX

MATHEMATICAL MODELING OF CELL DEATH

6.1 Introduction

Biofabrication processes including alginate gelation during laser-assisted cell printing may cause cell injury. Cell injury arises because of the normal/shear stress generated during the jet/microsphere formation process and during the jet/microsphere landing process. Additionally, the gelation process may alter the transmembrane (plasma membrane) ion gradients for the encapsulated cells and further aggravate the cell injury. Gelation process may also affect the availability of nutrients to the encapsulated cells during incubation and may influence the cell injury reversibility.

Mathematical modeling of relationship between operating conditions and cell responses is essential for evaluating the feasibility and efficiency of laser-assisted cell printing. However, intracellular biochemical reactions which are at the core of cell responses are very complex to quantify. As a result, alternative approaches are required for modeling the cell injury. In this chapter, mathematical expressions describing the relationship between operating conditions and cell injury are obtained using such alternative approaches.

6.2 Cell Injury Models

An overview of various mathematical models is outlined in this section. In the subsequent sections, process-induced cell injury is modeled using some of those models.

Finally, each model is compared with the experimental results to identify the model that better predicts the cell viability.

6.2.1 Power-law Models

The power-law model has been used initially to predict blood damage caused due to medical devices [Blackshear1965, Paul2003, Goubergrits2004, Grigioni2004]. The power-law function has the following general form:

$$I = C\tau^{b}t^{a} \qquad (6.1)$$

where I is the percentage of injured cells, τ is the mechanical stress experienced by the cells, and t is the time duration of the cells exposure to mechanical stress. C, b, and a are constant values for a given cell type and the process. The limitations of power-law model are it is not very accurate and it is not valid at large ranges of model input parameters. The percentage of injured cells exceeds 100% at large ranges of model input parameters which is not possible.

6.2.2 Gompertz Models

Gompertz model has been used to predict the populations of various multicellular organisms including fish and nematodes [Reznick2004, Fife2006, Minto2008]. A simple Gompertz function has the following general form [Reznick2004]:

$$V = \alpha e^{\beta x} \qquad (6.2)$$

where V is the population of the organisms, x is the model input parameter such as nutrition, and α and β are Gompertz constants. A complex Gompertz function has the following general form

$$I = A\exp(-Be^{CX}) \qquad (6.3)$$

where I is the percentage of injured organisms, X is the model input parameter such as the rate of viscous energy being dissipated by the fluid element and A, B, and C are Gompertz constants. The advantages of Gompertz function are it predicts populations accurately and it is valid even at large ranges of model input parameters. However, it has not been used at cellular level to predict percentage of injured cells in biofabrication processes.

6.2.3 Statistical Models

Process-induced cell injury, especially in orifice-based cell printing processes, has also been modeled using a probability density function [Li2010, Li2011a]. Under this approach, cell damage laws describing the relationship between cell injury and process parameters are established using a bivariate normal distribution function. The bivariate normal distribution function is a generalization of the one-dimensional normal distribution function to the two dimensions which is defined as:

$$f(s,t) = \frac{1}{2\pi\sigma_s\sigma_t\sqrt{1-\rho^2}}\exp\left[-\frac{z}{2(1-\rho^2)}\right] \qquad (6.4)$$

where $z \equiv \left(\frac{s-\mu_s}{\sigma_s}\right)^2 - 2\rho\left(\frac{s-\mu_s}{\sigma_s}\right)\left(\frac{t-\mu_t}{\sigma_t}\right) + \left(\frac{t-\mu_t}{\sigma_t}\right)^2$, μs and μt are mean values of stress s and exposure time t respectively. σs and σt are the standard deviations of s and t. ρ is the correlation coefficient between s and t. All fiver parameters are obtained experimentally. The overall process induced cell injury is defined as:

$$I(\tau, t) = \int\int f(\tau, t)\, d\tau dt \qquad (6.5)$$

where I is the percentage of cell injury. The main advantage of this model is that it is valid over large ranges of process parameters such as shear stress as it is based on probability theory. However, its main drawback is that it assumes normal distribution which may not be accurate.

6.2.4 Other Models

Process-induced cell injury in biofabrication processes has been modeled using a hybrid function of power-law and Gompertz functions [Li2011b]. The mathematical function has the following form:

$$I(\tau, T) = \frac{1}{1 + \tau^{-a} e^{-(bT+c)}} \qquad (6.6)$$

where I is the percentage of cell injury, τ is the shear stress, T is the temperature, a, b, c are model constants.

Molecular dynamic simulations have been used to study cell membrane in laser-assisted cell printing [Yin2011]. However, cell injury or cell death could arise because of mechanical stresses despite of intact cell membrane. Mechanical stresses could mechanically alter cell organelles such as proteins and cause cell death through apoptosis. Hence, molecular dynamic simulations do not capture process-induced cell injury effectively.

6.3 Mathematical Modeling of Process-induced Cell Death in Laser-assisted Cell Printing

Process-induced cell injury in this study is modeled using power-law and Gmpertz-models. A hybrid function of the form represented by Equation 5.6 is also used for modeling cell viability. However, predicted cell viability results did not match experimental results. A probability density function is not used for modeling because of its assumption of normal distribution. Experimental results indicate that cell viability decreases with increase in laser fluence and alginate concentration. Hence, laser fluence and sodium alginate concentration are used as the model input parameters.

Gelation time also affect the cell viability. However, the underlying physical and chemical interactions between cells and their extracellular environments are different for no gelation condition and two minutes gelation time. As a result, gelation time is not used as the model input parameter and distinct mathematical expressions are obtained for each gelation condition.

Cell viability data which is obtained after 24 hours post printing is used for deriving mathematical functions for predicting the post transfer encapsulated cell viability. Completion of apoptosis takes several hours and trypan blue assay used in this study could not detect cells in early stages of apoptosis because of their intact plasma membrane. As a result, cell viability data obtained immediately after printing, that is 0 hour, is not an accurate indicator of cell viability. Hence, incubation time is not used as the model input parameter.

The power law cell injury model used in this study is defined as follows:

$$I = k_1 \times L^{k_2} \times A^{k_3} \qquad (6.7)$$

where I is the model predicted cell injury in %, L is the model input laser fluence (mJ/cm2), A is the model input alginate concentration, and k1, k2 and k3 are the power-law model coefficients. The Gompertz cell injury model is defined as follows:

$$I = \exp(-k_4 \exp(-k_5 L - k_6 A)) \times 100 \qquad (6.8)$$

where k4, k5, and k6 are Gompertz constants.

To understand which model better predicts the cell viability, model prediction error is calculated and is defined as follows:

$$E = \sqrt{\frac{\sum_{i=N}^{N} (x_i - \bar{x})^2}{N-1}} \qquad (6.9)$$

where $x_i = e_i - p_i$, ei is the experimental cell viability, pi is model predicted cell viability, and $\bar{x}$ is mean of xi.

6.4 Results and Discussion

All equation coefficients are determined based on the mean cell injury experimental results using non-linear least-squares data fitting with Matlab. The data fitting codes and results are documented in Appendix A. The equation coefficients for no gelation and two-minute gelation condition are summarized in Table 6.1.

Table 6.1: Model coefficients

Coefficient	Gelation condition	
	No gelation	2 min gelation
$k_1 (cm^2)^{-k2}.(mJ)^{k2}.(ml)^{-k3}.(g)^{k3}$	0.002054	0.068709
k_2	1.234831	-0.09912
k_3	0.719503	-0.00143
K_4	4.436989	12.45907
$K_5 (cm^2)^{-1}.(mJ)$	0.000495	0.000728
$K_6 (ml)^{-1}.(g)$	0.179957	0.655481

For no gelation condition, cell viability as a function of varying laser fluence and 1% (w/v) constant alginate concentration is shown in Figure 6.1. As seen Figure 6.1, power-law model and Gompertz model predicted cell viabilities decrease with increase in laser fluence. As laser fluence increases, jet/droplet formation acceleration increases, and consequently the jet/droplet landing deceleration increases, generating larger normal/shear stress, which results in lower cell viability [Wang2008, Lin2009b, Lin2010]. As result, cell viability decreases with increase in laser fluence. Hence, power-law and Gompertz predictions for varying laser fluence are in agreement with experimental observations and previous studies [Lin2009b, Lin2010].

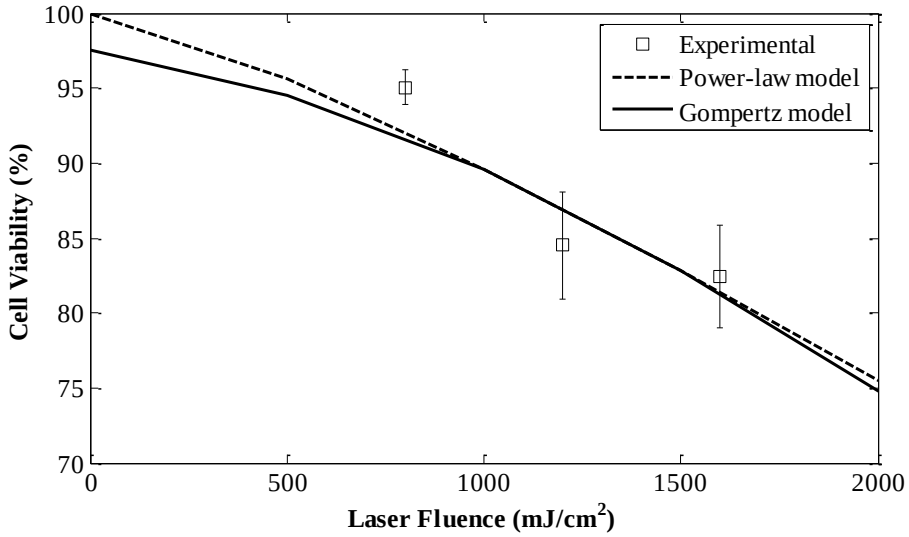

Figure 6.1: Cell viability as a function of varying laser fluence and 1% (w/v) constant alginate concentration for no gelation condition

For no gelation condition, cell viability as a function of constant laser fluence 800 mJ/cm^2 and varying alginate concentration is shown in Figure 6.2. From figure 6.2, power-law model and Gompertz model predicted cell viabilities decrease with increase in alginate concentration. Viscosity of sodium alginate solution increases with sodium alginate concentration [Khalil2006, Gruene2011D, Lin2009a]. Consequently, the stress generated during the jet/droplet formation process increases due to more stretches in polymer chains with higher sodium alginate concentration, which could decrease the cell viability.

Meanwhile, both the acceleration and deceleration generated during the jet/droplet formation and landing process decreases due to increase in bioink viscosity, which could increase the cell viability. From experimental results, it appears, increase in stress generated during the jet/droplet formation process outweighs the decrease in acceleration and deceleration generated during the jet/droplet formation and landing process due to

increase in bioink viscosity. As a result, cell viability decreases with increase alginate concentration. Thus, power-law and Gompertz predictions for varying alginate concentration are in agreement with experimental observations.

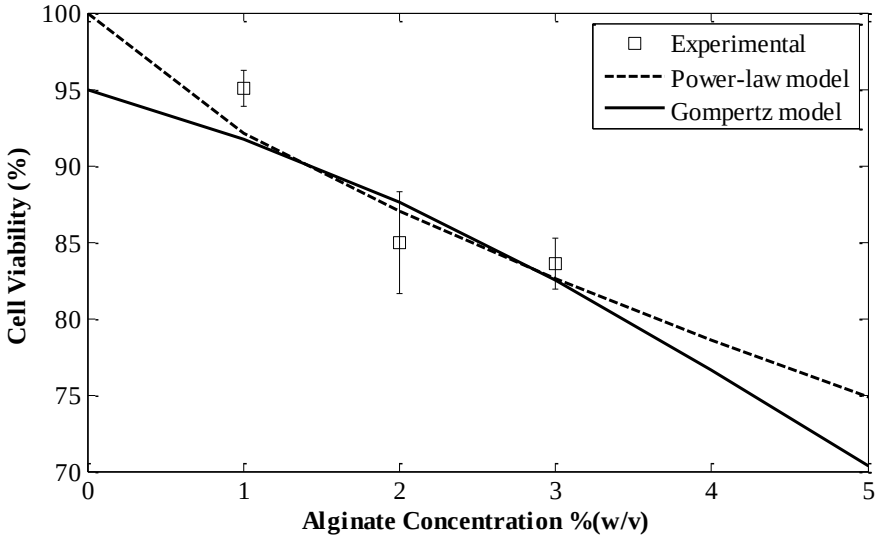

Figure 6.2: Cell viability as a function of constant laser fluence 800 mJ/cm^2 and varying alginate concentration for no gelation condition

Figure 6.3 shows cell viability as a function of varying laser fluence and 1% (w/v) constant alginate concentration for two-minute gelation condition. Despite the cushion effect of the gel membrane during jet/droplet landing, landing deceleration increases with increase in laser fluence. As a result, cell viability decreases with increase in laser fluence for cells subjected to gelation. As depicted in Figure 6.3, power-law model and Gompertz model predicted cell viabilities under varying laser fluence are in agreement with experimental observations and previous studies [Lin2009b, Lin2010].

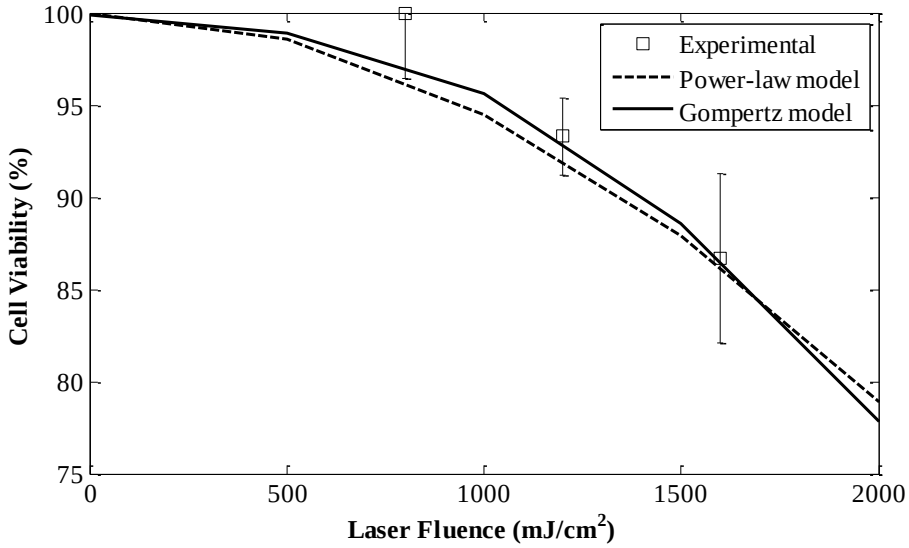

Figure 6.3: Cell viability as a function of varying laser fluence and 1% (w/v) constant alginate concentration for two-minute gelation condition

Figure 6.4 shows cell viability as a function of constant laser fluence 800 mJ/cm^2 and varying alginate concentration for two-minute gelation condition. For the cells subjected to gelation, an increase in sodium alginate concentration results in a smaller microsphere with thinner gel membrane, which increases combined diffusion coefficient (Dm) [Lin2011] [Chai2004]. At the same time, an increase in sodium alginate concentration will also results in a more dense gel structure, which decreases Dm [Chai04]. The two factors also compete with each other [Chai2004]. However, the diameter of the microsphere decreases only less than 5% when sodium alginate concentration increases from 2% to 3% [Lin2011], which does not have much influence on both the combined diffusion coefficient (Dm) and gel structure.

As a result, the effect of sodium alginate concentration on combined diffusion coefficient is less significant. Thus, even though pore diameter of the gelled alginate microspheres decreases with sodium alginate concentration [Yao2012], it does not have

much influence on cell viability for either calcium ion influx or nutrition influx when encapsulated cells are exposed to calcium chloride solution (after printing) or DMEM medium (during incubation). Hence, the decreasing trend of post-transfer cell viabilities for cells subjected to either gelation or no gelation is attributed to the competing effect of process-induced mechanical stresses. Therefore, power-law and Gompertz predictions for varying alginate concentration are in agreement with experimental observations.

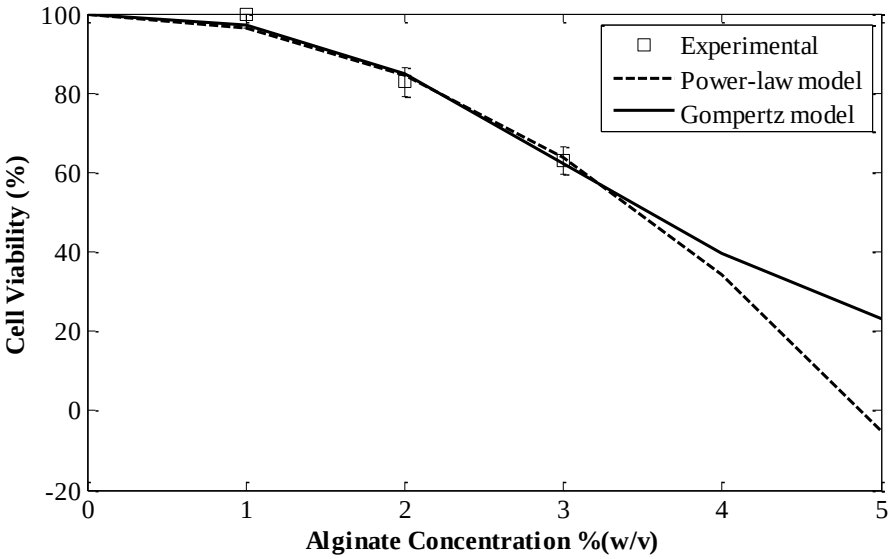

Figure 6.4: Cell viability as a function of constant laser fluence 800 mJ/cm^2 and varying alginate concentration for two-minute gelation condition.

Overall, the power-law prediction error is 2.08 whereas Gompertz prediction error is 2.04. However, power-law model predicted cell viability assumes a large negative value at large laser fluences or alginate concentrations as shown in Figure 4. In contrast, Gompertz predicted cell viability simply approaches zero and it never assumes a negative value even at large ranges of model input parameters. Cell viability should be always

positive and hence, Gompertz model is more appropriate for predicting cell viability than power-law model in laser-assisted cell printing.

6.5 Summary

Process-induced injury during alginate gelation in laser-assisted cell printing is modeled using power-law and Gompertz models. Important conclusions are:

1) Gompertz model can be used at cellular level to model process-induced injury in biofabrication processes.
2) Gompertz model and power-law model prediction errors are nearly equal. However, Gompertz model is more appropriate for predicting cell viability because of its validity at large values of model input parameters.

CHAPTER SEVEN

CONCLUSIONS AND FUTURE WORK

7.1 Conclusions

As a preliminary study towards the cell injury in laser-assisted 3D cell printing, this study serves to investigate the effect of alginate gelation, gelation time, alginate concentration, and the effect of operating conditions such as the laser fluence on post-transfer cell viability during laser-assisted cell printing. In this study, sodium alginate and calcium chloride are used as the gel precursor and gel reactant solution to facilitate alginate gelation. Two experimental setups are used for assessing the effects of various parameters in laser-assisted printing process on cell viability.

Experimental setup A is used for investigating the effects of gelation, gelation time as well as laser fluence on cell viability. In Experimental setup A, a single concentration of sodium alginate in bioink which is 1% (w/v) is used. The laser fluences used are 800, 1200, and 1600 mJ/cm^2. Two receiving substrate solutions, which are 2% (w/v) calcium chloride solution and DMEM culture medium, are used for each of the three laser fluences. Alginate microspheres printed into the calcium chloride solution underwent gelation whereas alginate microspheres printed into DMEM media did not undergo gelation. The incubation periods used are 0 hour and 24 hours after printing.

Experimental setup B is used for examining the effect of sodium alginate concentration on cell viability. In Experimental setup B, two different sodium alginate concentrations in bioink are used which are 2% and 3% (w/v). A laser fluence of 800 mJ/cm^2 is used for printing the bioink. Either 2% (w/v) calcium chloride solution or

DMEM medium were used as the receiving substrate same as in Experimental setup A. The incubation periods used were 0 hour and 24 hours after printing.

Post transfer, the printed cells are subjected to either two-minute gelation or ten-minute gelation time through interaction with calcium chloride. Two-minute gelation time is one in which printed alginate droplets are allowed to interact with calcium chloride for two minutes after printing. Contrastingly, ten-minute gelation is one in which printed alginate droplets are allowed to interact with calcium chloride for approximately 10 minutes. In certain instances, the printed alginate microspheres are not subjected gelation at all, in order to better understand the impact of gelation process on cell viability. The cell viability for the printed cells is assessed immediately after the printing as well as after 24 hours post printing. Important observations and conclusions are outlined below:

1) Alginate gelation at the receiving substrate increases the viability of the cells subjected to gelation because of the cushioning effect of the gel membrane which minimizes the normal/shear stress generated during the microsphere impact.

2) Longer the gelation time or the duration for which sodium alginate droplets interact with calcium chloride solution, the lower is the viability of the cells. A long gelation time increases the alginate microsphere gel membrane thickness which reduces the osmosis of oxygen and nutrients to the encapsulated cells during incubation. Also, cell injury due to Ca^{2+} ions is greater. As a result, a long gelation time prevents cell injury repair and causes death of injured cells.

3) Increase in laser fluence decreases the viability of the cells subjected to gelation. The decrease cell viability with laser fluence is caused due to the combining effect of the mechanical stress generated during the jet/droplet formation process as well as the calcium ions diffusion into the microspheres. The mechanical stress increases with increase in laser fluence which increases cell injury. Contrastingly, calcium ions diffusion decreases with increase laser fluence which decreases cell injury. Overall, the mechanical stress has a dominating effect on cell injury than calcium ions diffusion. As a result, cell viability decreases with laser fluence for cells subjected to gelation.

4) Increase in alginate concentration decreases the viability of the cells subjected to gelation or no gelation. The decreasing trend of post-transfer cell viabilities for cells subjected to gelation or no gelation with alginate concentration is due to the competing effect of process-induced mechanical stresses. The mechanical stress generated during the jet/droplet formation process increases due to more stretches in polymer chains with higher sodium alginate concentration, which decreases the cell viability. On the other hand, both the acceleration and deceleration generated during the jet/droplet formation and landing process decreases due to increase in bioink viscosity, which increases the cell viability. The mechanical stress generated during the jet/droplet formation process has a dominating effect on cell viability than the acceleration and deceleration generated during the jet/droplet formation and landing process. Even though pore diameter of the gelled alginate microspheres decreases with alginate concentration [Yao2012], it does not have

much influence on cell viability for either calcium ion influx or nutrition influx when encapsulated cells are exposed to calcium chloride solution (after printing) or DMEM medium (during incubation). Hence, cell viability decreases with increase in alginate concentration.

5) Based on experimental data, power-law model and Gompertz model based mathematical functions are derived to predict cell viability for the post-transfer cells after 24 hours of incubation. Gompertz model better predicts cell viability than power-law model.

7.2 Future Work

Effect of alginate gelation on cell viability in laser-assisted cell printing is investigated in this study. Mathematical modeling of relationship between operating conditions and cell responses is essential for evaluating the feasibility and efficiency of laser-assisted cell printing. However, cellular signaling pathways which guide the cell responses, shown in figure 7.1, are ignored in this study.

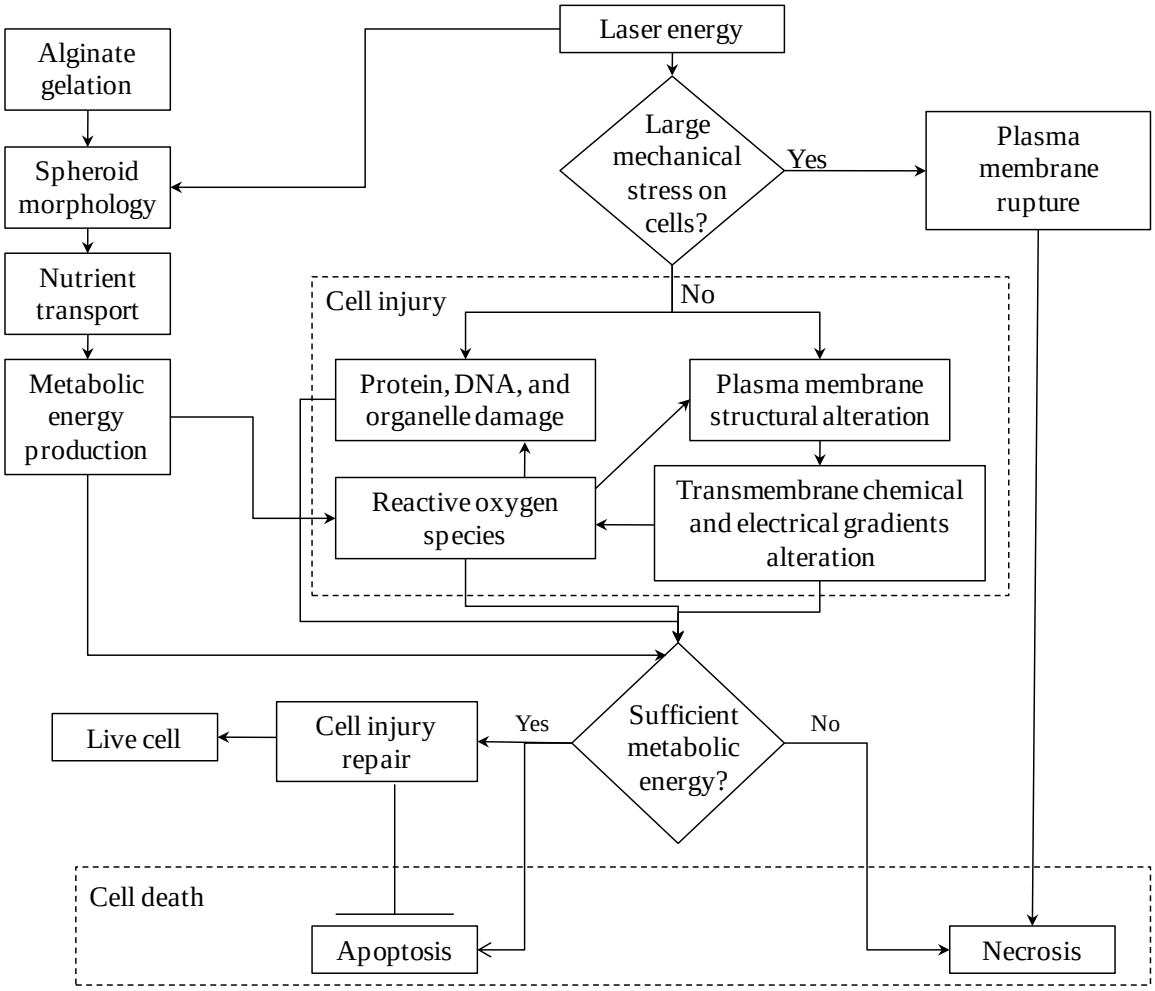

Figure 7.1: Cellular responses to operating conditions in laser-assisted cell printing

As shown in Figure 7.1, laser pulses when focused on to the quartz disk, eject jets/droplets of bioink into the receiving substrate. Mechanical stress is generated during the jet/droplet formation and landing processes [Barron2004c, Hopp2005b]. If the mechanical stress is sufficiently large, it instantaneously ruptures plasma membrane and causes cell death through necrosis. Contrastingly, if the mechanical stress is small, it does not injure the cells. However, if the mechanical stress is intermediate, it mechanically alters plasma membrane, proteins, DNA, and other organelles.

The mechanical disruption of plasma membrane results in alteration of transmembrane chemical and electrical gradients, especially calcium ion gradient when calcium chloride is used as the receiving substrate. The alteration of transmembrane calcium ion gradient results in generation and accumulation of reactive oxygen species (ROS) in cells. ROS are in general, are produced as an unavoidable by product during metabolic energy production in cells. ROS accumulation further damages plasma membrane, proteins, DNA, and other organelles, thus triggering a vicious cycle.

Meanwhile, laser energy and alginate concentration influence the morphology of the cell-laden microspheres. The morphology of the microspheres governs the transport of nutrients and oxygen into the microspheres which consecutively governs the metabolic energy production in cells. Cell injury repair and cell death are governed by metabolic energy that is available to the cells [Agarwal2005, Kumar2005]. When metabolic energy is not sufficient, injured cells eventually die of necrosis. However, if sufficient metabolic energy is available, cell injury repair and apoptotic pathways are simultaneously activated.

Apoptosis is activated through intrinsic pathway because cells of immune system are absent in vitro conditions to activate extrinsic pathway as shown in Figure 6.2. In case the injured cells are able to repair the injury before the inhibitors apoptosis are completely saturated with proapoptotic proteins, then intrinsic pathway of apoptosis is deactivated and injured cells will be alive. If the injured cells are not able to repair the injury before the inhibitors apoptosis are completely saturated with proapoptotic proteins, then the proapoptotic proteins completes apoptosis and causes cell death.

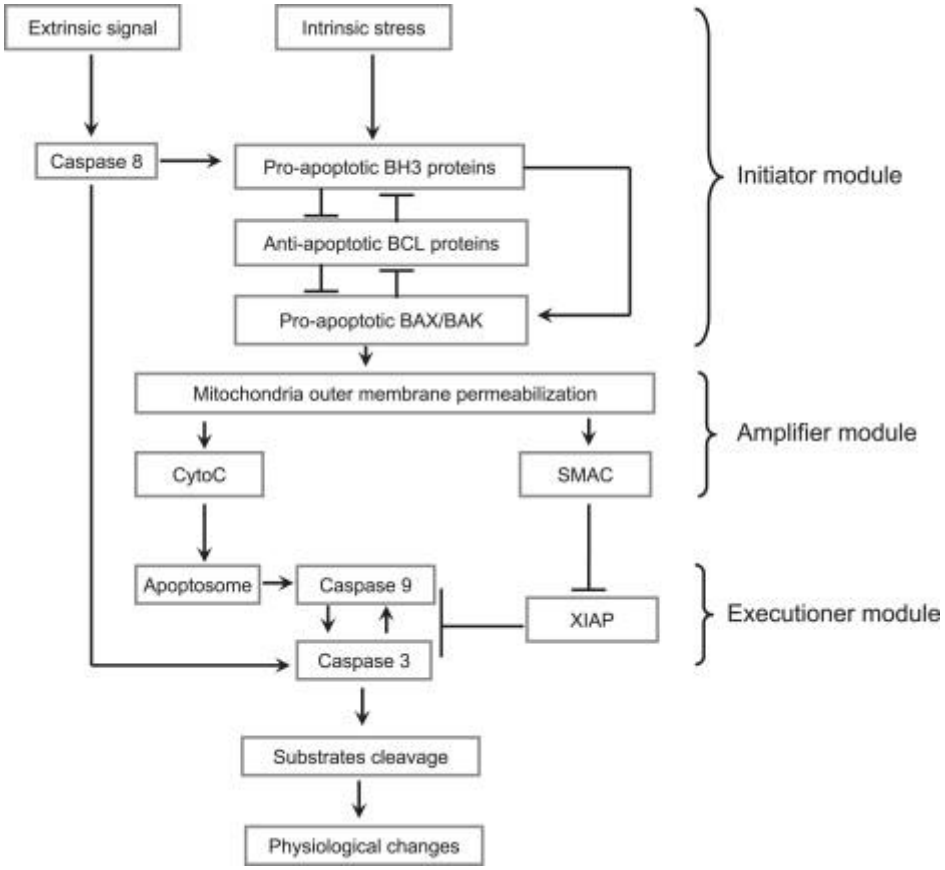

Figure 7.2: Intrinsic pathway of apoptosis [Zhang2009]

Trypan blue assay was used in this study for detecting dead cells. However, it has several limitations. One is, it can wrongly detect alive cells as dead cells when then their plasma membrane integrity is temporarily compromised. Other is, it can wrongly detect cells in early apoptosis as live cells because of their intact plasma membrane. Future studies on laser-assisted cell printing should incorporate assays that are capable of detecting apoptosis and necrosis, especially immediately after printing, to better understand cellular responses to operating condition. Additionally, assays capable of detecting proapoptotic proteins of intrinsic as well as extrinsic pathways should be used

in future to confirm apoptosis occurs only though intrinsic pathway. Furthermore, mathematical models based on intracellular molecular signaling pathways should be developed in future for accurately predicting cell viability. Propagation of error is not considered in final cell viability values in this study [Figliola2011]. Thus, future studies have to include error propagation in final cell viability values.

APPENDICES

Appendix A

Power-law Model Matlab Codes

A.1 Power-law Model Function Code

```
function [F] = poweri(k,x)
F = k(1).*(x(:,1).^k(2)).*(x(:,2).^k(3));
end
```

A.2 Power-law Function Execution Code

A.2.1 No Gelation Condition

```
load PowerNoData.txt
x(:,1)=PowerNoData(:,1);
x(:,2)=PowerNoData(:,2);
y(:,1)=PowerNoData(:,3);

k0=[1 0 0 4.95084733];
[k,error]=lsqcurvefit(@poweri,k0,x,y)
```

A.2.2 Two Minutes Gelation Time

```
load Power2Data.txt
x(:,1)=Power2Data(:,1);
x(:,2)=Power2Data(:,2);
y(:,1)=Power2Data(:,3);

k0=[1 0 0 0];
[k,error]=lsqcurvefit(@poweri,k0,x,y)
```

A.3 Text File Data

A.3.1 PowerNoData Text File Data

800	1	4.95084733
1200	1	15.49129375
1600	1	17.57031947

800	2	15.06762526
800	3	16.42955642

A.3.2 Power2Data Text File Data

800	1	0
1200	1	6.701287765
1600	1	13.31440499
800	2	17.17692747
800	3	37.04753292

Appendix B

Gompertz Model Matlab Codes

B.1 Gompertz Model Function Code

```
function [F] = gompertz(k,x)
F=(exp(-k(1).*exp((-k(2).*(x(:,1)))+(-k(3).*(x(:,2))))))*100;
End
```

B.2 Gompertz Function Execution Code

B.2.1 No Gelation Condition

```
load GompertzNoData.txt

x(:,1)=GompertzNoData(:,1);
x(:,2)=GompertzNoData(:,2);
y(:,1)=GompertzNoData(:,3);

k0=[0 0 0 4.95084733];
[k,error]=lsqcurvefit(@gompertz,k0,x,y)
```

B.2.2 Two Minutes Gelation Time

```
load Gompertz2Data.txt

x(:,1)=Gompertz2Data(:,1);
x(:,2)=Gompertz2Data(:,2);
y(:,1)=Gompertz2Data(:,3);

k0=[ 0 0 0 0];
[k,error]=lsqcurvefit(@gompertz,k0,x,y)
```

B.3 Text File Data

B.3.1 GompertzNOdata Text File Data

800 1 4.95084733

1200	1	15.49129375
1600	1	17.57031947
800	2	15.06762526
800	3	16.42955642

B.3.2 Gompertz2Data Text File Data

800	1	0
1200	1	6.701287765
1600	1	13.31440499
800	2	17.17692747
800	3	37.04753292

REFERENCES

[Agarwal2005] Agarwal, J., Walsh, A., Peters, S., and Lee, R.C., 2005, "Multimodal Strategies for Resuscitating Injured Cells," Ann. NY. Acad. Sci., vol.1066, pp.295–309.

[Alberts2008] Alberts, B., Johnson, A., Lewis, J., Raff, M., Roberts, K., and Walter, P, 2008, Molecular Biology of the Cell, 5th ed., Garland Science, New York, NY.

[Aguado2011] Aguado, B.A., Mulyasasmita, W., Su, J., Lampe, K.J., and Heilshorn, S.C., 2011, "Improving viability of stem cells during syringe needle flow through the design of hydrogel cell carriers," Tissue Eng. Part A, vol.18(7–8), pp. 806–815.

[Ashkenazi2002] Ashkenazi, A., 2002, "Targeting Death and Decoy Receptors of the Tumour-Necrosis Factor Superfamily," Nat. Rev. Cancer, vol.2(6), pp.420–430.

[Baehrecke2011] Baehrecke, E. H., 2011, "The Grand Finale," Cell, Vol.144(4), pp. 463-464.

[Bagci2006] Bagci, E.Z., Vodovotz, Y., Billiar, T.R., Ermentrout, G.B., and I. Bahar. 2006. Bistability in Apoptosis: Roles of Bax, Bcl-2, and Mitochondrial Permeability Transition Pores. Biophys. J. 90: 1546-1559.

[Barron2004a] Barron, J.A., Ringeisen, B.R., Kim, H., Spargo, B.J., and Chrisey, D.B., 2004, "Application of Laser Printing to Mammalian Cells," Thin Solid Films, vol.453-454, pp.383-387.

[Barron2004b] Barron, J.A., Wu, P., Ladouceur, H.D., and Ringeisen, B.R., 2004, "Biological Laser Lrinting: a Novel Technique for Creating Heterogeneous 3-dimensional Cell Patterns," Biomed. Microdevices, vol.6(2), pp.139-147.

[Barron2004c] Barron, J.A., Spargo, B.J., and Ringeisen, B.R., 2004, "Biological Laser Printing of Three Dimensional Cellular Structures," Appl. Phys., vol.79(4-6), pp.1027-1030.

[Barron2005] Barron, J.A., Krizman, D.B., and Ringeisen, B.R., 2005, "Laser Printing of Single Cells: Statistical Analysis, Cell Viability, and Stress," Ann. Biomed. Eng., vol.33(2), pp.121-130.

[Bartolo2007] Bartolo, D., Boudaoud, A., Narcy, G., and Bonn, D., 2007, "Dynamics of Non-Newtonian Droplets," Phys. Rev. Lett. vol.99(17), pp.174502-1-174502-4.

[Bernardi2007] Bernardi, P., and Rasola, A., 2007, "Calcium and Cell Death: the Mitochondrial Connection," Subcell. Biochem., vol.45, pp.481–506.

[Bischof2005] Bischof, J.C., and He, H., 2005, "Thermal Stability of Proteins," Ann. NY. Acad. Sci., vol.1066, pp.12–33.

[Blackshear1965] Blackshear, P.L., Dorman, F.D., and Steinbach, J.H., 1965, "Some Mechanical Effects that Influence Haemolysis," Trans. Am. Soc. Artif. Intern. Organs, vol.11(1), pp.112-117.

[Blandino1999] Blandino, A., Macias, M., and Cantero, D., 1999, "Formation of Calcium Alginate Gel Capsules: Influence of Sodium Alginate and CaCl2 Concentration on Gelation Kinetics," J. Biosci. Bioeng., vol.88(6), pp.686–689.

[Cao2012] Cao, N., Chen, X. B.,and Schreyer, D. J., 2012, "Influence of Calcium Ions on Cell Survival and Proliferation in the Context of an Alginate Hydrogel," ISRN Chemical Engineering, vol.2012.

[Campanella2004] Campanella, M., Pinton, P., Rizzuto, R., 2004, "Mitochondrial Ca2+ Homeostasis in Health and Disease," Biol. Res., vol.37(4), pp.653–660.

[Catros2011] Catros, S., Guillotin, B., Baca´kova´ , M., Fricain, J.C., and Guillemot, F., 2001, "Effect of Laser Energy, Substrate Film Thickness and Bioink Viscosity on Viability of Endothelial Cells Printed by Laser-assisted Bioprinting," Appl. Surf. Sci., vol.257(12), pp. 5142–5147.

[Chai2004] Chai, Y., Mei, L. H., Lin, D. Q., and Yao, S. J.,2 004, "Diffusion Coefficients in Intrahollow Calcium Alginate Microcapsules," J. Chem. Eng. Data, vol.49(3), pp.475–478.

[Csipo1998] Csipo, I., Montel, A. H., Hobbs, J. A., Morse, P. A., and Brahmi, Z., 1998, "Effect of Fas+ and Fas- Target Cells on the Ability of NK Cells to Repeatedly Fragment DNA and Trigger Lysis via the Fas Lytic Pathway," Apoptosis, vol.3(2), pp.105-114.

[Doraiswamy2006] Doraiswamy, A., Narayan, R., and Lippert, T., 2006, "Excimer Laser Forward Transfer of Mammalian Cells Using a Novel Triazene Absorbing Layer," Appl. Surf. Sci., vol.252(13), pp.4743-4747.

[Doraiswamy2007] Doraiswamy, A,. Narayan, R.J., Harris, M.L., Qadri, S.B., Modi, R., and Chrisey, D.B., 2007, "Laser Microfabrication of Hydroxyapatite-osteoblast-like Cell Composites," J. Biomed. Mater. Res., vol.80(3), pp.635-643.

[Eguchi1997] Eguchi, Y., Shimizu, S., and Tsujimoto, Y., 1997, "Intracellular ATP levels determine cell death fate by apoptosis or necrosis," Cancer Research, vol.57(10), pp. 1835–1840.

[Fedorovich2011] Fedorovich, N.E., Kuipers, E., Gawlitta, D., Dhert, W.J., and Alblas, J., 2011, "Scaffold Porosity and Oxygenation of PrintedHydrogel Constructs Affect Functionalityof Embedded Osteogenic Progenitors," Tissue Engineering Part A., vol.17(19-20), pp.2473-2486.

[Fife2006] Fife, J.P., Ozkan, H.E., Derksen, R.C., and Grewal, P.S., 2006, "Using Computational Fluid Dynamics to Predict Damage of a Biological Pesticide during Passage through a Hydraulic Nozzle," Biosystems Engineering, vol.94(3), pp.387–396.

[Figliola2011] Figliola, R.S., and Beasely, D.E, 2011, Theory and Design for Mechanical Measurements, 5th ed., John Wiley and Sons, Hoboken, NJ.

[Fulda2006] Fulda, S., and Debatin, K.M., "Extrinsic Versus Intrinsic Apoptosis Pathways in Anticancer Chemotherapy," Oncogene, vol.25(34), pp.4798–4811.

[Fussenegger2000] Fussenegger, M., Bailey, J.E., and Varner, J., 2000, "A Mathematical Model of Caspase Function in Apoptosis," Nat. Biotechnol. vol.18, pp.768–774.

[Galluzzi2008] Galluzzi, L., and Kroemer, G., 2008, "Necroptosis: A Specialized Pathway of Programmed Necrosis," Cell, vol.135(7), pp.1161–1163.

[Giansanti2011] Giansanti, V., Torriglia, A., and Scovassi, A,I., 2011, "Conversation Between Apoptosis and Autophagy: "It is your turn or mine?"," Apoptosis, vol.16(4), pp.321 – 333.

[Giersiepen1990] Giersiepen, M., Wurzinger, L.J., Opitz, R., and Reul, H., 1990, "Estimation of Shear Stress Related Blood Damage in Heart Valve Prosthese: in Vitro Comparison of 25 Aortic Valves," Int. J. Artif. Organs, 13(5), pp.300-306.

[Giorgi2008] Giorgi, C., Romagnol,i A., Pinton, P., and Rizzuto, R., 2008, "Ca2+ Signaling, Mitochondria and Cell Death," Curr. Mol. Med, vol.8(2), pp.119–130.

[Gissel2005] Gissel, H., 2005, "The Role of Ca2+ in Muscle Cell Camage," Ann. NY. Acad. Sci., vol.1066, pp.166–180.

[Gissel2011] Gissel, H., Lee, R. C., and Gehl, J., 2011, "Electroporation and Cellular Physiology," Clinical Aspects of Electroporation, vol.423, pp.9-17.

[Goubergrits2004] Goubergrits, L., and Affeld, K., 2004. "Numerical Estimation of Blood Damage in Artificial Organs," Artif. Organs, vol.28(5), pp.499–507.

[Grigioni2004] Grigioni, M., Daniele, C., Morbiducci, U., D'Avenio, G., Di Benedetto, G., and Barbaro, V., 2004, "The Power-law Mathematical Model for Blood Damage Prediction: Analytical Developments and Physical Inconsistencies,"Artif. Organs.,vol.28(5), pp.467–475.

[Gross2007] Gross, J.D., Constantinidis, I., and Sambanis, A., 2007, "Modeling of Encapsulated Cell Systems," J. Theor. Biol., vol.244(3), pp.500-510.

[Gruene2011a] Gruene, M., Pflaum, M., Hess, C., Diamantouros, S., Schlie, S., Deiwick, A., Koch, L., Wilhelmi, M., Jockenhoevel, S., Haverich, A., and Chichkov, B.N., 2011, "Laser Printing of 3-D Multicellular Arrays for Studies of Cell–cell and Cell–environment Interactions," Tissue. Eng. Part C, vol.17(10), pp.973– 982.

[Gruene2011b] Gruene, M., Deiwick, A., Koch, L., Schlie, S., Unger, C., Hofmann, N., Bernemann, I., Glasmacher, B., and Chichkov, B., 2011, "Laser Printing of Stem Cells for Biofabrication of Scaffold-free Autologous Grafts," Tissue Engineering Part C: Methods, 17(1), pp.79-87.

[Gruene2011c] Gruene, M., Pflaum, M., Deiwick, A., Koch, L., Schlie, S., Unger, C., Wilhelmi, M., Haverich, A., Chichkov, B., 2011, "Adipogenic Differentiation of Laserprinted 3D Tissue Grafts Consisting of Human Adipose-derived Stem Cells," Biofabrication, vol.3(1).

[Gruene2011d] Gruene, M., Unger, C., Koch, L., Deiwick, A., and Chichkov, B., 2011, "Dispensing Pico to Nanolitre of a Natural Hydrogel by Laser-assisted Bioprinting," Biomed Eng Online, vol.10.

[Guillotin2010] Guillotin, B., Souquet, A., Catros, S., Duocastella, M., Pippenger, B., Bellance, S., Bareille, R., Rémy, M., Bordenave, L,, Amédée , J., and Guillemot, F., 2010, "Laser Assisted Bioprinting of Engineered Tissue with High Cell Density and Microscale Organization," Biomaterials, vol.31, pp.7250-7256.

[Guillotin2011] Guillotin, B., and Guillemot, F., 2011, "Cell Patterning Technologies for Organotypic Tissue Fabrication," Trends Biotechnol, vol.29, pp.183-90.

[Guo2005] Guo, W., Shea, J., Berry, R., 2005, "The Physics of the Interactions Governing Folding and Association of proteins," Ann. NY. Acad. Sci., vol.1066, pp.34–53.

[Harsdorf1999] Harsdorf, R., Li, P., and Dietz, R., 1999, "Signaling pathways in reactive oxygen species-induced cardiomyocyte apoptosis", Basic Science Report, vol.99, pp. 2934-2941.

[Hennings1980] Hennings, H., Michael, D., Cheng, C., Steinert, P., Holbrook, K., and Yuspa, S. H., 1980, "Calcium Regulation of Growth and Differentiation of Mouse Epidermal Cells in Culture," Cell, vol.19(1), pp.245–254.

[Henriquez2008] Henriquez, M., Armisen, R., Stutzin, A., Quest, A.F., 2008, "Cell Death by Necrosis, a Regulated Way to Go," Curr. Mol. Med., vol.8(3), pp.187–20.

[Hitomi2008] Hitomi, J., Christofferson, D.E., Ng, A., Yao, J., Degterev, A., Xavier, R.J., and Yuan, J., 2008, "Identification of a Molecular Signaling Network that Regulates a Cellular Necrotic Cell Death Pathway," Cell, vol.135(7), pp.1311–132.

[Hopp2005a] Hopp, B., Smausz, T., Kresz, N., Barna, N., Bor, Z., Kolozsva´ri, L., Chrisey, D., Szabo´, A., and No´gradi, A., 2005, "Survival and Proliferative Ability of Various Living Cell Types After Laser-induced Forward Transfer," Tissue. Eng., vol.11, pp.1817-1823.

[Hopp2005b] Hopp, B., Smausz1, T., Barna, N., Vass, C.S., Antal, Z.S., Kredics, L., and Chrisey, D., 2005, "Time-resolved Study of Absorbing Flm Assisted Laser Induced Forward Transfer of Trichoderma Longibrachiatum Conidia," J. Phys. D: Appl. Phys., vol.38(6), pp.833–837.

[Hwang 2010] Hwang, C. M., Sant, S.,Masaeli, M., Kachouie, N. N., Zamanian, B., Lee, S. H., Khademhosseini, A., 2010, " Fabrication of ThreeDimensional Porous Cell-Laden Hydrogel for Tissue," Biofabrication, vol.2(3).

[Kampinga2006] Kampinga, H. H., 2006, "Chaperones in Preventing Protein Denaturation in Living Cells and Protecting Against Cellular Stress," Handb. Exp. Pharmacol.,vol.172, pp.1–42.

[Kao2005] Kao, J., Rosenstein, B.S., Peters, S., Milano, M.T., and Kron, S.J., 2005, "Cellular Response to DNA Damage," Ann. NY. Acad. Sci., vol.1066, pp.243–258.

[Kattamis2007] Kattamis, N.T., Purnick, P.E., Weiss, R., and Arnold, C.B., 2007, "Thick Film Laser Induced Forward Transfer for Deposition of Thermally and Mechanically Sensitive Materials," Appl. Phys. Lett. , vol.91(17), pp.171120-71123.

[Khalil2006] Khalil, S., 2006, “Deposition and Structural Formation of 3D Alginate Tissue Scaffolds,” Ph.D thesis, Drexel University.

[Koch2009] Koch, L., Kuhn, S., and Sorg, H, 2009, “Laser Printing of Skin Cells and Human Stem Cells,” Tissue Eng. Part C Methods, vol.16(5), pp.847-854.

[Kroemer2009] Kroemer, G., Galluzzi, L., Vandenabeele, P., Abrams, J., Alnemri, E.S., Baehrecke, E.H., 2009, “Classification of Cell Death: Recommendations of The Nomenclature Committee on Cell Death,” Cell Death Differ., vol.16(1), pp.3–11.

[Kumar2005] Kumar, V., Abbas, A., Fausto, N., 2005, Robbins & Cotran Pathologic Basis of Disease, 7th ed., Saunders, Philadelphia, PA.

[Kulka2006] Engelberg-Kulka, H., Amitai, S., Kolodkin-Gal, I., and Hazan, R., 2006, “Bacterial Programmed Cell Death and Multicellular Behavior in Bacteria,” PLoS Genet., vol.2(10), pp.1518-1526.

[Langer1993] Langer, R., and Vacanti, J., 1993, “Tissue Engineering,” Science, vol.260, pp.920–926.

[Lee1992] Lee, G.M., Han, B.K., Kim, J.H., and Palsson, B.O., 1992, "Effect of Calcium Chloride Treatment on Hybridoma Cell Viability and Growth," Biotechnology Letters, vol.14(10), pp.891-896.

[Li2010] Li, M., Tian, X., Zhu, N., Schreyer, D.J., and Chen, X., 2010, “Modeling process-induced cell damage in the biodispensing process,” Tissue Eng. Part C Methods, vol.16(3), pp.533-542.

[Li2011a] Li, M., Tian, X., Schreyer, D. J., and Chen, X., 2011, “Effect of Needle Geometry on Fow Rate and Cell Damage in the Dispensing-based Biofabrication Process,” Biotechnol. Prog.,vol. 27(6), pp.1777–1784.

[Li2011b] Li, M., Tian, X., and Chen X., 2011, “Temperature effect on the shearinduced cell damage in biofabrication,” Artif. Organs, vol.35(7), pp741–746.

[Lin2009a] Lin, Y., Huang, Y., and Chrisey, D.B., 2009, "Droplet Formation in Matrix-assisted Pulsed-laser Evaporation direct Writing of Glycerol-water Solution," J. Appl. Phys., vol. 105, pp. 093111.

[Lin2009b] Lin, Y., Huang, Y., Wang, G., Tzeng, J., and Chrisey, D.B., 2009, “Effect of Laser Fluence on Yeast Cell Viability in Laser-assisted Cell Transfer”, Journal of Applied Physics, vol.106(4), pp.043106-1-7.

[Lin2010a] Lin, Y., Huang, G., Huang, Y., Tzeng, T.R.J., and Chrisey, D.B., 2010, "Effect of Laser Fuence in Laser-assisted Direct Writing of Human Colon Cell," Rapid Prototyping J.,vol.16, pp.202–208.

[Lin2010b] Lin, Y., 2010, "Pulsed-Laser Direct Writing of Biological Materials," Ph.D thesis, Clemson University.

[Lin2011] Lin, Y., and Huang, Y., 2011,"Laser-Assisted Fabrication of Highly Viscous Alginate Microsphere," J. of Applied Physics, vol.109(8), pp. 083107-1-8.

[Majno1995] Majno, G., and Joris, I., 1995, "Apoptosis, Oncosis and Necrosis: An Overview of Cell Death," Am. J. Pathol., vol.146(1), pp.3-15.

[Mammarella2003] Mammarella, E.J., and Rubiolo, A.C, 2003, "Crosslinking Kinetics of Cation-hydrocolloid Gels," Chem. Eng. J., vol.94(1), pp.73–77.

[Martino2011] Martino, N.A., Lange-Consiglio, A., Cremonesi, F., Valentini, L., Caira, M., Guaricci, A.C, Ambruosi, B., Sciorsci, R.L., Reshkin, S.J, and Dell'Aquila, M.E, 2011, "Functional Expression of the Extracellular Calcium Sensing Receptor (CaSR) in Equine Umbilical Cord Matrix Size-Sieved Stem Cells," PLoS ONE, vol.6(3), e17714.

[Mayr2002] Mayr, M., Hu, Y., Hainaut, P., and Xu, Q., 2002, "Mechanical stress-induced DNA damage and racp38MAPK signal pathways mediate p53-dependent apoptosis in vascular smooth muscle cells", vol.16, pp. 1423-1425.

[McGinnis1999] McGinnis, K.M., Wang, K.W., and Gnegy, M.E, 1999, "Alternations of Extracellular Calcium Elicit Selective Modes of Cell Death and Protease Activation in SHSY5Y Human Neuroblastoma Cells," J. Neurochem., vol.72(5), pp.1853–1863.

[McNeil1998] McNeil, S.E., Hobson, S.A., Nipper, V., and Rodland, K.D., 1998, "Functional Calcium Sensing Receptors in Rat Fibroblasts are Required for Activation of SRC Kinase and Mitogen-activated Protein Kinase in Response to Extracellular Calcium," J. Biol. Chem., vol.273(2), pp.1114–1120.

[Minto2008] Minto, C., Myers, R.A., and Blanchard, W., 2008, "Survival Variability and Population Density in Fish Populations," Nature, vol.452, pp.344–347.

[Mironov2009] Mironov, V., Viconti, R.P., Kasyanov, V., Forgacs, G., Drake, C.J, and Markwald, R.R., 2009, "Organ Printing: Tissue Apheroids as Building Blocks," Biomaterials, vol.30(12), pp.2164-2174.

[Moquin2010] Moquin, D., and Chan, F. K., 2010, "The Molecular Regulation of Programmed Necrotic Cell Injury," Trends in Biochem. Sci., vol.35(8), pp.434-441.

[Nair2009] Nair, K., Gandhi, M., Khalil, S., Yan, K.C., Marcolongo, M., Barbee, K., and Sun, W., 2009, "Characterization of Cell Viability during Bioprinting Processes," Biotechnol J., vol.4(8), pp.1168–1177.

[Nishiyama2009] Nishiyama, Y., Nakamura, M., Henmi, C., Yamaguchi, K., Mochizuki, S., Nakagawa, H., and Takiura, K., 2009, "Development of a Three-dimensional Bioprinter: Construction of Cell Supporting Structures Using Hydrogel and State-of-the-art Inkjet Technology," Journal of Biomechanical Engineering, vol.131, pp.035001-1-035001-6.

[Ochieng1991] Ochieng, J., Tahin, Q. S., Booth, C. C., and Russo, J., 1991, "Buffering of Intracellular Calcium in Response to Increased Extracellular Levels in Mortal, Immortal, and Transformed Human Breast Epithelial Cells," J. Cell Biochem., vol.46(3), pp.250–254.

[Orgill2005] Orgill, D.P., Porter, S.A., and Taylor, H.O., 2005, "Heat Injury to Cells In Perfused Systems," Ann. NY. Acad. Sci., vol.1066, pp.106-118.

[Orrenius2003] Orrenius, S., Zhivotovsky, B., and Nicotera, P., 2003, "Regulation of Cell Death: The Calcium-apoptosis Link," Nat. Rev. Mol. Cell. Biol.,vol.4(7), pp.552–565.

[Ovsianikov2010] Ovsianikov, A., Gruene, M., Pflaum, M., Koch, L., Maiorana, F., Wilhelmi, M., Haverich, A., and Chichkov, B., 2010, "Laser Printing of Cells Into 3D Scaffolds," Biofabrication, vol.2, pp.014104.

[Patz2006] Patz, T.M., Doraiswamy, A., Narayan, R.J., He, W., Zhong, Y., Bellamkonda, R., Modi, R., and Chrisey, D. B. , 2006, "Three-dimensional Direct Writing of B35 Neuronal Cells," J. Biomed. Mater. Res. B Appl. Biomater., vol.78B(1), pp.124-130.

[Paul2003] Paul, R., Apel, J., Klaus, S., Schügner, S., Schwindke, P., and Reul, H., 2003, "Shear Stress Related Blood Damage in Laminar Couette Flow," Artificial Organs, vol.27(6), pp.517–529.

[Rezende2007] Rezende, R.A., Bartolo, .J., Mendes, A., and Filho, R.M., 2007, "Experimental Characterisation of the Alginate Gelation Process for Rapid Prototyping," Chemical Engineering, vol.11, pp.509-514.

[Reznick2004] Reznick, D.N., Bryant, M.J., Roff, D., Ghalambor, C.K., and Ghalambor, D.E., 2004, "Effect of Extrinsic Mortality on the Evolution of Senescence in Guppies," Nature, vol.431, pp.1095–1099.

[Ringeisen2002] Ringeisen, B.R., Wu, P.K., Kim, H., Pique, A., Auyeung, R.Y., Young, H.D., Chrisey, D.B., and Krizman. D.B., 2002, " Picoliter-scale Protein Microarrays by Laser Direct Write," Biotechnol. Prog., vol.18(5), pp.1126-1129.

[Ringeisen2004] Ringeisen, B.R., Kim, H., Barron, J.A., Krizman, D.B., Chrisey, D.B., Jackman, S., Auyeung, R.Y., and Spargo, B.J., 2004, "Laser Printing of Pluripotent Embryonal Carcinoma Cells," Tissue Eng., VOL.10(3-4), PP.483-491.

[Simon2000] Simon, H., Yehia, A., and Schaffer, F., 2000, "Role of reactive oxygen species (ROS) in apoptosis induction", Apoptosis, vol.5, pp. 415-418.

[Vos2008] Vos, M.J., Hageman, J., Carra, S., and Kampinga, H., 2008, "Structural and Functional Diversities Between Members of the Human HSPB, HSPH, HSPA, and DNAJ Chaperone Families," Biochemistry, vol.47(27), pp.7001–7011.

[Wang2008] Wang, W., Huang, Y., Grujicic, M., and Chrisey, D.B., 2008,"Study of Impact-Induced Mechanical Effects in Cell Direct Writing Using Smooth Particle Hydrodynamic Method," ASME J. of Manufacturing Sci. and Eng., vol. 130(2), pp. 021012-1-10.

[Xu2012] Xu, C., Chai, W., Huang, Y., and Markwald, R.R., 2012, "Scaffold-free Inkjet Printing of Three-dimensional Zigzag Cellular Tubes," Biotechnol. Bioeng.

[Xu2013] Xu, T., Zhao, W., Zhu, J.M., Albanna, M.Z., Yoo, J.J., and Atala, A., 2013, "Complex Heterogeneous Tissue Constructs Containing Multiple Cell Types Prepared by Inkjet Printing Technology," Biomaterials, vol.34(1), pp.130-139.

[Yan2012] Yan, J., Huang, Y., and Chrisey, D.B., "Laser-Assisted Printing of Alginate Long Tubes and Annular Constructs," Biofabrication, Accepted.

[Yao2012] Yao, R., Zhang, R., Luan, J., and Lin, F., 2012, "Alginate and Alginate/gelatin Microspheres for Human Adipose-derived Stem cell Encapsulation and Differentiation," Biofabrication, vol.4(2).

[Yin2011] Yin, J., and Huang, Y., 2011, "Study of Process-Induced Cell Membrane Stability in Cell Direct Writing," ASME J. of Manufacturing Sci. and Eng., vol. 133(5), pp. 054501-1-5.

[Zhang2009] Zhang, T., Brazhnik, P., and Tyson, J.J., 2009, "Computational Analysis of Dynamical Responses to the Intrinsic Pathway of Programmed Cell Death," Biophys. J., vol.97(2), pp.415-434.

[Zhivotovsky2011] Zhivotovsky, B., and Orrenius, S., 2011, "Calcium and Cell Death Mechanisms: A Perspective from the Cell Death Community," Cell Calcium, vol.50(3), pp.211-221.